Article

Not peer-reviewed version

Sea Cucumber (*Isostichopus badionotus*): Bioactivity and Wound Healing Capacity In Vitro of Small Peptide Isolates from Digests of Whole-Body Wall or Purified Collagen

Leticia Olivera-Castillo *, George Grant *, Oscar Medina-Contreras, Honorio Cruz-López, Leydi Carrillo-Cocom, Ariadnna Cruz-Córdova, Frank Segura-Cadiz, Daniel Alejandro Fernández-Velasco, Sergio Rodríguez-Morales, Juan V. Cauich-Rodríguez, Rosa Moo-Puc Esther Moo-Puc, César Puerto-Castillo Puerto-Castillo, Gabrielas de Jesu Moo-Pech, Jonatan Jafet Uuh-Narvaez, Miguel Ángel Olvera-Novoa, Rossanna Rodriguez-Canul

Posted Date: 18 September 2025

doi: 10.20944/preprints202509.1539.v1

Keywords: Holothuroid; body wall proteins; collagen; bioactive peptides; small molecular weight peptides; wound healing in vitro

Article

Sea Cucumber (*Isostichopus badionotus*): Bioactivity and Wound Healing Capacity In Vitro of Small Peptide Isolates from Digests of Whole-Body Wall or Purified Collagen

Leticia Olivera-Castillo [1,*], George Grant [2,*], Oscar Medina-Contreras [3], Honorio Cruz-López [4], Leydi Carrillo-Cocom [5], Ariadnna Cruz-Córdova [6], Frank Segura-Cadiz [1], Daniel Alejandro Fernández-Velasco [7], Sergio Rodríguez-Morales [8], Juan Valerio Cauich-Rodríguez [9], Rosa Esther Moo-Puc [10,11], César Puerto-Castillo [1], Gabriela de Jesus Moo-Pech [12], Jonatan Jafet Uuh-Narvaez [5], Miguel Ángel Olvera-Novoa [1] and Rossanna Rodriguez-Canul [1]

[1] Departamento Recursos del Mar, Centro de Investigación y de Estudios Avanzados del IPN, Unidad Mérida (Cinvestav), Antigua Carretera a Progreso Km. 6, 97310 Merida, Yucatan, Mexico
[2] Independent Researcher, Aberdeen, UK
[3] Hospital Infantil de México Federico Gómez, 162 Doctor Marquez, Col. Doctores, Alcaldía Cuauhtémoc, 06720 Ciudad de México, Mexico
[4] Escuela Nacional de Estudios Superiores Unidad Mérida (ENES Mérida), Universidad Nacional Autónoma de México, Ucú México
[5] Facultad de Ingeniería Química, Universidad Autónoma de Yucatán, Periférico Norte Km. 33.5, Chuburná de Hidalgo Inn, 97203 Merida, Yucatan, Mexico
[6] Laboratorio de Investigación en Inmunoquímica., Hospital Infantil de Mexico Federico Gómez, Calle Doctor Márquez 162, Col. Doctores, Alcaldía Cuauhtémoc, 06720 Ciudad de México, México
[7] Laboratorio de Fisicoquímica e Ingeniería de Proteínas, Departamento de Bioquímica, Facultad de Medicina, Universidad Nacional Autónoma de México, Ciudad Universitaria, Alcaldía Coyoacán, 04510 Ciudad de México, México
[8] Unidad de Química en Sisal, Facultad de Química, Universidad Nacional Autónoma de México, Puerto de Abrigo S/N, Sisal, Hunucmá, Yucatan, Mexico
[9] Centro de Investigación Científica de Yucatán, Unidad de Materiales, Calle 43 No. 130 x 32 y 34, Col. Chuburná de Hidalgo, 97205 Merida, Yucatan, Mexico
[10] Secretaría de Ciencia, Humanidades, Tecnología e Innovación - Hospital Regional de Alta Especialidad de la Península de Yucatán, IMSS-Bienestar, Calle 20 No. 119, Fracc. Altabrisa, 97130 Merida, Yucatan, Mexico
[11] Ciencia y Herbolaria, Calle 1 # 122, San Jose Kuche, 97345 Conkal, Yucatan, Mexico
[12] Instituto Tecnólogico de Mérida, Av. Tecnólogico s/n Km 4.5, 97118 Merida, Yucatan, Mexico
* Correspondence: loliveracastillo@gmail.com (L.O.-C.); george.grant63@gmail.com (G. G)

Abstract

Low-molecular-weight peptides derived by digestion of body wall proteins from some sea cucumber species have wound-healing and health-promoting properties. Sea cucumber body composition varies widely by species, growth environment, age and season, so it is unknown if all species contain the requisite bioactive peptides. For the first time, small peptide (1-3 kDa) fractions have been isolated from the whole-body wall of the sea cucumber *Isostichopus badionotus* and its constituent collagen, and tested for wound healing capacity in vitro. The body wall comprised around 50% collagen, whose composition and structure were like, but not identical to, other sea cucumber collagens. Ultrafiltered digests (1-3 kDa) of the pure collagen and a further purified fraction of it, as well as a 1-3 kDa digest of whole-body wall, had potent antioxidant activities and promoted rapid wound healing in a keratinocyte scratch wound assay. Gene expression studies suggested that the wound-healing actions of the individual 1-3 kDa fractions differed significantly. Low-molecular-weight peptides derived

 doi:10.20944/preprints202509.1539.v1

from *I. badionotus* collagen did promote wound healing in vitro, however, their efficacy may have been modulated by additional factors produced during body wall or collagen digestion.

Keywords: Holothuroid; body wall proteins; collagen; bioactive peptides; small molecular weight peptides; wound healing in vitro

1. Introduction

Sea cucumbers (Holothuroidea: Echinodermata) are benthic marine animals found in intertidal zones and shallow environments of the sea floor. Worldwide, there are at least 1,770 known species of sea cucumbers of which around 80 are intensively fished and harvested for use as health-promoting foodstuffs or as sources of nutraceuticals [1–3].

Sea cucumbers have a remarkable capacity for regeneration after damage to or loss of internal organs, including the digestive tract [4,5]. For this reason, they are a source of many metabolism-modulating and potentially health-promoting factors, such as saponins, glycosaminoglycans, chondroitin sulfate, sulfated polysaccharides, fucoidan, phenolics, lectins, cerebrosides, sterols, and bioactive peptides [6–8]. The content and potency of these constituents can vary significantly depending on species, growth environment, physiological/stress state, and handling or processing of captured or harvested animals [9–11].

Much recent study has centred on bioactive peptides produced during the digestion of sea cucumber body wall proteins, including collagen, the main proteinaceous component of the body wall. Reports indicate that these peptides have anticancer, antihypertensive, immune-enhancing, brain-modulating, and wound-healing properties in vitro and in vivo [7,8,12,13].

Sea cucumber *Isostichopus badionotus* is distributed primarily in the Caribbean Sea and along the Western Atlantic Ocean coast, including off the Yucatan Peninsula of Mexico. Studies have shown that this species' body wall contains bioactive factors, including glycosaminoglycans, fucoidins, and proteinaceous components that can ameliorate or block inflammation and modulate cellular metabolism in potentially beneficial health-promoting ways, both in vitro and in vivo [8,14,15].

The health-modulating properties of low-molecular-weight, or small, peptides from *I. badionotus* have not been evaluated to date. In the present study, collagen from *I. badionotus* was isolated and characterised. Then, 1-3 kDa fractions of digests of pure collagen and whole-body wall were collected and tested for bioactivity and the ability to promote wound healing in a scratch wound assay.

2. Results

2.1. Composition of I. badionotus

The moisture content of the skin-free body wall of *I. badionotus* was 800 g kg^{-1} wet body weight. On a dry weight basis, its ash content was 400 g kg^{-1}, lipid content was 200 g kg^{-1}, and protein content was 330 g kg^{-1}. Collagen comprised approximately 50% of body wall protein and 60% of that collagen was in the form of intact fibrils.

2.2. Preliminary Study

Low-molecular-weight compounds produced during enzymatic digestion of sea cucumber body wall are reported to have anti-inflammatory and wound-healing properties in vitro and in vivo [7,8]. The level and potency of these factors can vary significantly depending on the species, region, environment, growth conditions, and storage and handling after collection. To establish whether enzymatic digests of *I. badionotus* captured off the coast of Yucatan, Mexico, possessed significant wound-healing properties, a preliminary study was conducted in which three ultrafiltrate fractions were obtained from enzymatic (papain) digestion of the body wall (BW): < 1 kDa BW, 1-3 kDa BW and > 3 kDa BW. This preliminary wound healing evaluation indicated that the 1-3 kDa ultrafiltrate

 doi:10.20944/preprints202509.1539.v1

fraction of digested *I. badionotus* skin-free body wall was a potent promoter of wound healing over 24 hours in a scratch assay based on HaCat cells (Figure 1a). In contrast, significant wounds remained on control medium plates as well as plates treated with the <1 kDa BW or >3 kDa BW fractions.

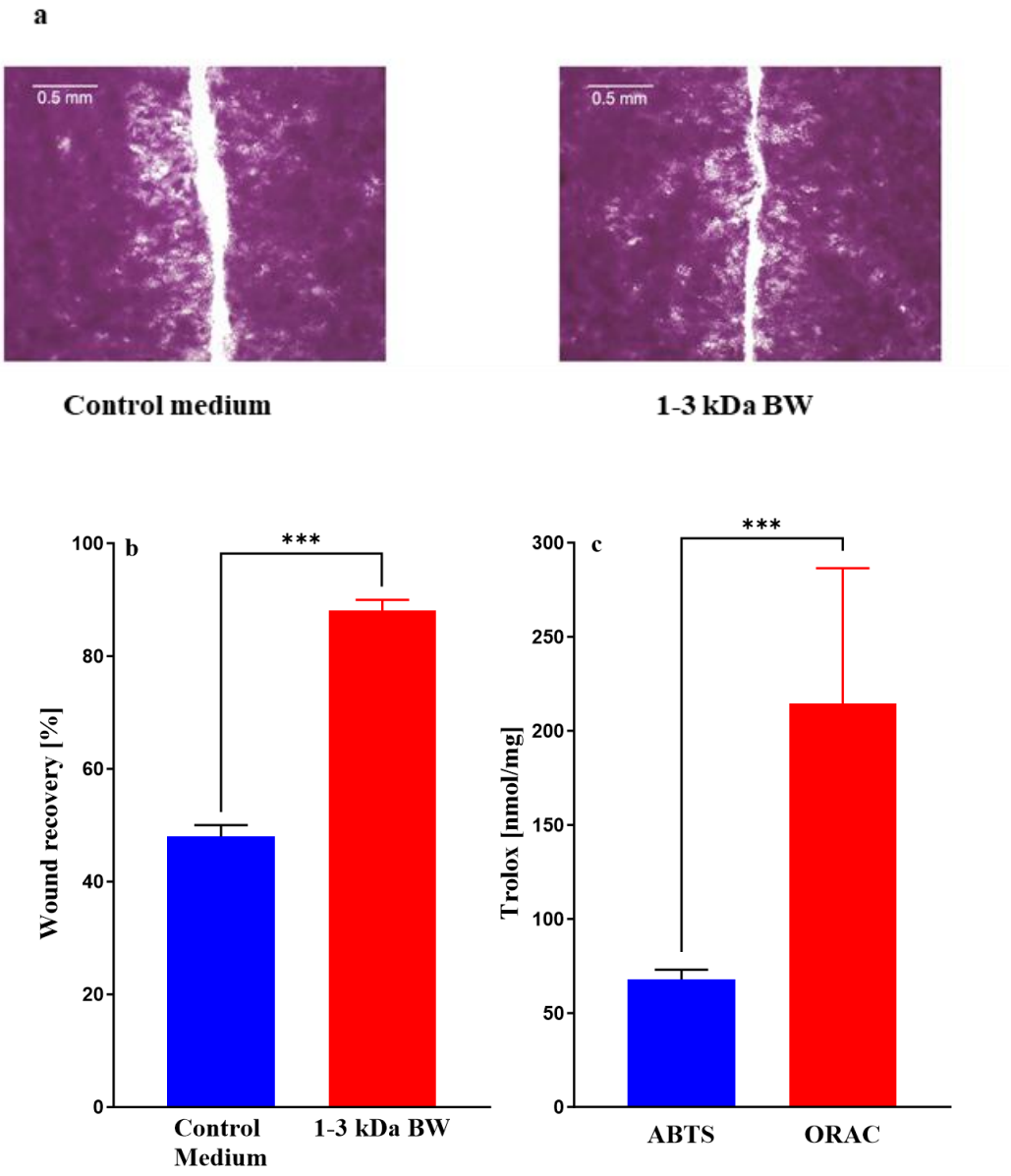

Figure 1. Images (a) and evaluations (b) of wound healing in a scratch assay based on human keratinocytes cultured for 24 h in media containing 10% foetal calf serum with or without ultrafiltrate fractions of digested body wall from *I. badionotus* (1-3 kDa BW) and the constituent antioxidant activities (ABTS and ORAC) for 1-3 kDa BW (c). For each data set, *** indicates a significant difference ($p \leq 0.001$).

The 1-3 kDa BW ultrafiltrate was active in both ABTS and ORAC antioxidant assays (Figure 1b). However, the potencies differed significantly, with the Trolox equivalent activity in the ORAC assay being approximately four-fold higher than in the ABTS assay.

The antibacterial activity of the *I. badionotus* preparation was tested against *Escherichia coli* ATCC 25922, *Pseudomonas aeruginosa* ATCC 13637, *Pseudomonas aeruginosa* 64D (MDR), *Staphylococcus aureus* ATCC 25725, *Staphylococcus aureus* MR (Methicillin resistant), *Enterococcus faecalis* ATCC 51299 (Vancomycin resistant) and *Enterococcus faecium* 683D (Vancomycin resistant). Bacteria were grown in Mueller-Hinton broth, and $5x10^5$ CFU/mL were inoculated in Mueller-Hinton medium with or without extract at different concentrations by serial two-fold dilutions: 0.125 mg/mL to 4 mg/mL. No

 doi:10.20944/preprints202509.1539.v1

growth was observed in bacteria evaluated in this study after incubating at 4 mg/mL for 18 h at 37 °C. To verify absence of growth, 10 µL were later plated out on Blood agar or Luria Bertani agar. Significant growth was evident with *Staphylococcus aureus* ATCC 25725, *Staphylococcus aureus* MR (Methicillin-resistant), *Enterococcus faecalis* ATCC 51299 (Vancomycin-resistant) and *Enterococcus faecium* 683D (Vancomycin-resistant), but not with *Escherichia coli* ATCC 25922, *Pseudomonas aeruginosa* ATCC 13637, or *Pseudomonas aeruginosa* 64D (MDR). These findings indicate that, at a concentration of 4 mg/mL, *I. badionotus* was bacteriostatic against the Gram-positive bacteria, but bactericidal against the Gram-negative bacteria.

2.3. Collagen Isolation and Characterisation

Collagen is the principal protein component of the sea cucumber body wall. As a result of our preliminary finding that skin-free *I. badionotus* body wall digest had potent wound healing capacity and 50% of its body protein was collagen [two thirds as intact fibrils], this body wall constituent was isolated by pepsin-digestion and characterised by scanning electron microscopy (SEM), electrophoresis (SDS-PAGE), amino acid analysis, Fourier transform infrared spectroscopy (FTIR), x-ray diffraction (XRD), and circular dichroism (CD).

2.3.1. Scanning electron microscope

Scanning electron microscope (SEM) images of the collagen samples obtained by pepsin-digestion of *I. badionotus* show well-developed fibril networks with thin, relatively uniform and densely interwoven fibrils of collagen consistent with a homogeneously clustered network (Figure 2).

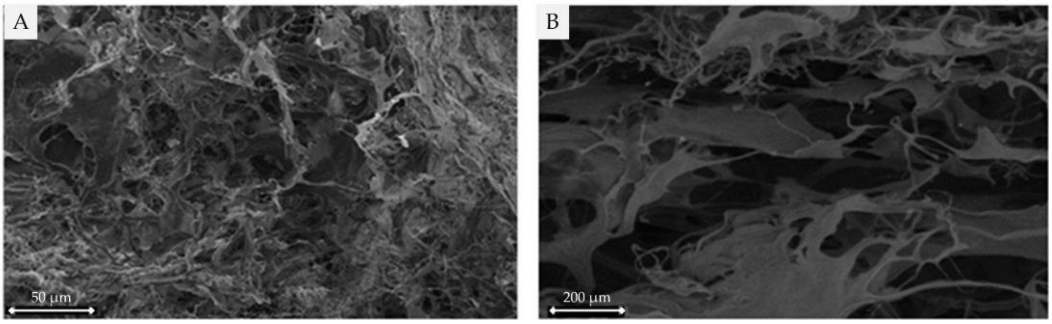

Figure 2. Scanning electron microscope (SEM) images of pepsin-soluble collagen from *I. badionotus* by secondary electrons (A) and by retro-disperse electrons (B).

2.3.2. SDS-PAGE

Electrophoresis (SDS-PAGE) revealed that collagen isolates from *I. badionotus* body wall consisted primarily of an α chain [~131 kDa], but also contained small amounts of a β chain [~ 220 kDa] (Figure 3). No small-molecular-weight impurity bands were evident, indicating that the molecular structure of the collagen was not destabilised or degraded during processing and extraction.

 doi:10.20944/preprints202509.1539.v1

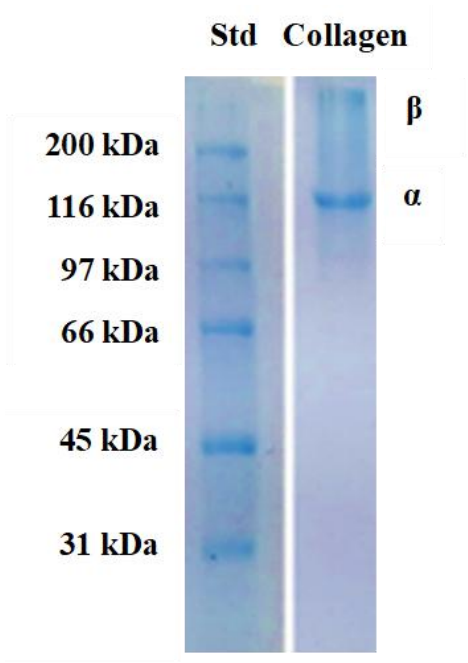

Figure 3. SDS-PAGE electrophoresis in reduced conditions of collagen from *I. badionotus* body wall. (Std: SDS-PAGE molecular weight standards broad range (Bio-Rad) 6.5 kDa to 200 kDa).

2.3.3. Amino acid composition

The amino acid composition of the collagen extracted from *I. badionotus* body wall shows glycine (Gly) to be the most abundant amino acid, followed by glutamic acid (Glu), alanine (Ala), hydroxyproline (Hyp), proline (Pro), and arginine (Arg) (Table 1). Histidine (His), methionine (Met), hydroxylysine (Hyl), lysine (Lys), isoleucine (Ile), leucine (Leu), and tyrosine (Tyr) were low content, and cysteine (Cys) was present in trace amounts. The imino acids (Pro+Hyp) comprised 17.2 per cent of residues in the collagen preparation.

Table 1. Amino acid composition of pepsin-soluble collagen from skin-free body wall of *I. badionotus*.

Amino acid	Residues*	Amino acid	Residues*
Aspartic acid	93	Tyrosine	6
Glutamine	157	Valine	20
Hydroxyproline	97	Methionine	5
Serine	21	Cysteine	1
Glycine	289	Isoleucine	10
Histidine	3	Leucine	15
Arginine	54	Hydroxylysine	5
Threonine	23	Phenylalanine	9
Alanine	110	Lysine	5
Proline	75	Imino acids**	172

*Residues/1000 residues. ** Proline+Hydroxyproline.

2.3.4. UV-visible spectra and Fourier transform infrared spectroscopy.

Collagen extracted from *I. badionotus* body wall showed a strong primary absorption band at 226 nm (Figure 4a), similar to fish collagen (*Totoaba macdonaldi*). There was an additional small absorption band at 258 nm, corresponding to amino acids with aromatic rings (Phe and Tyr), indicating a low

 doi:10.20944/preprints202509.1539.v1

content of these amino acids. This finding aligns with the amino acid profile and further confirms the purity of the extracted collagen.

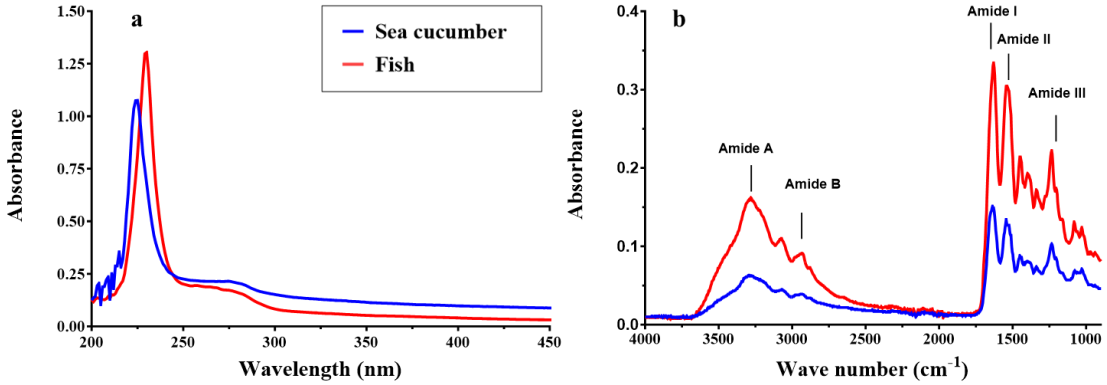

Figure 4. UV-visible spectra (a) and Fourier transform infrared spectroscopy (FTIR) (b) of collagen from skin-free body wall of *I. badionotus* collagen and from the fish *Totoaba macdonaldi*. .

Collagen extracted from *I. badionotus* body wall and fish collagen showed similar and characteristic absorption bands in FTIR spectroscopy (Figure 4b). These were assigned as amide A (3295 cm^{-1}), amide B (2933 cm^{-1}), amide I (1636 cm^{-1}), amide II (1543 cm^{-1}), and amide III (1234 cm^{-1}). These bands are comparable with the FTIR spectra of collagen from marine species; amide A represents the stretching vibrations of N–H and C–H, and amide B that of –NH. Amide I represents C = O stretching vibrations coupled with N–H bending vibrations, CN stretching, and CCN deformation. The presence of amide I bands in the 1600–1660 cm^{-1} range indicates the presence of a triple-helical structure. The bending vibration of N–H coupled to C–N is represented by the amide II band, which predicts the characteristic peaks of protein secondary structures. The amide III band indicates a complex mix of α-helices and β-sheets along with a random coil of the protein structure. Furthermore, the ratio between amide III and pyrrolidine ring (band at 1450 cm^{-1}) vibration of proline and hydroxyproline was around 1.06, indicative of a triple helical structure for collagen from *I. badionotus* body wall.

2.3.5. Circular dichroism and x-ray diffraction

Circular dichroism (CD) is an efficient spectroscopy technique for confirming the structural integrity of the collagen triple helix. The collagen from *I. badionotus* body wall exhibited a weak positive absorption peak at 220 nm, and a negative one at 195 nm (Figure 5a). This indicates it is similar to that of other sea cucumber species and in line with the FTIR spectra (Figure 4b); that is, it had an intact triple helical structure. Temperature-induced unfolding of this structure exhibited a monophasic change in ellipticity at 222 nm (Figure 5b). The estimated denaturation temperature (Td) for collagen from *I. badionotus* body wall was 32.5 °C . In sea cucumber collagens, Td is variable, but the value recorded for *I. badionotus* was at the high end of the range (32.3 to 34.6 °C). Elevated Tds have been linked to high imino acid content in collagens. In the present study, *I. badionotus* collagen had an imino acid content of 172 residues/1000 residues, which is comparable to that for collagens of similar thermal stability. By contrast, sea cucumber collagens with lower imino acid contents have Tds as low as 17.9-18.5 °C.

 doi:10.20944/preprints202509.1539.v1

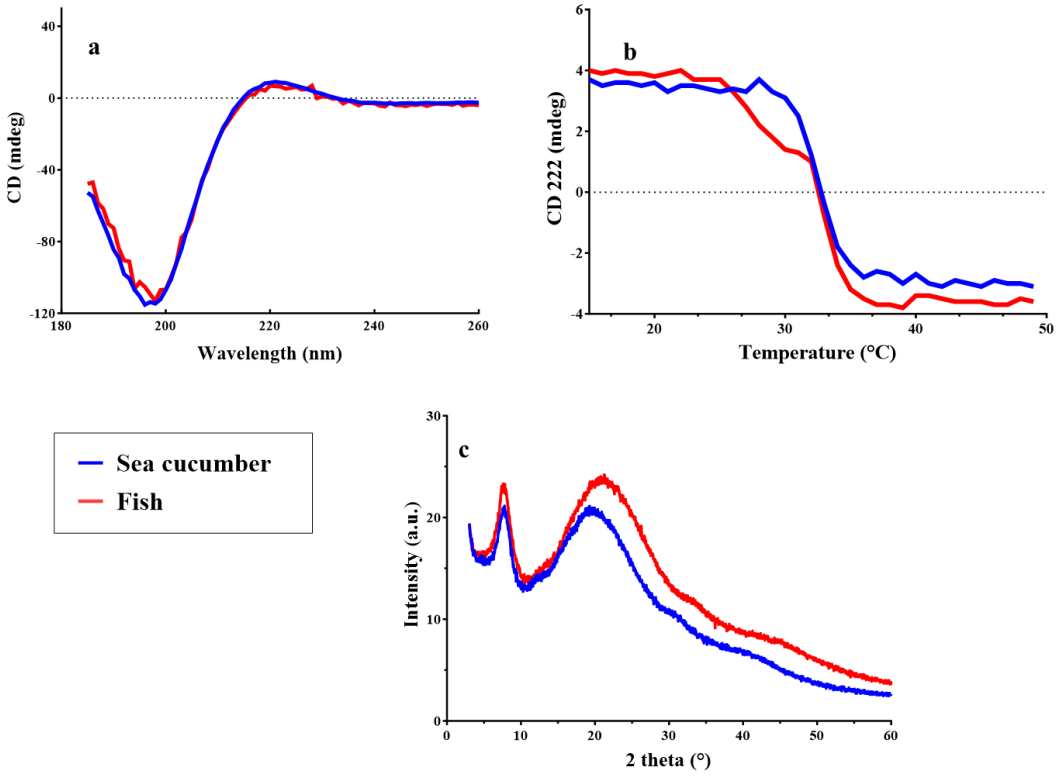

Figure 5. Far-UV circular dichroism spectra (a), temperature-induced unfolding followed at 222 nm (b) and x-ray diffraction (XRD) (c) of collagen from *I. badionotus* and from the fish *Totoaba macdonaldi*.

The *I. badionotus* collagen XRD pattern exhibits clear reflections corresponding to an amorphous natural polymer (protein) as indicated by the presence of two peaks similar to the fish (*T. macdonaldi*) collagen (Figure 5c). One sharp peak appears at 2θ=7.9° with a broad peak observed with a 2θ=20.0° maximum, as reported previously [27,28]. The sharp peak can be assigned to triple helix molecular chains with a separation distance of 1.12 nm as calculated with Bragg's law. For the broad peak (disordered collagen chains), chain distance was reduced up to 0.44 nm. This implies that the collagen contains ordered triple helix chains with a large chain separation as well as disordered collagen chains with smaller distances.

2.3.6. Collagen hydrolysis and ultrafiltration

Collagen fibres were solubilised from *I. badionotus* body wall with pepsin, salted out, recovered by centrifugation, dialysed and lyophilised. The fibrils were then digested with papain. The digestate was filtered and centrifuged. The degree of hydrolysis (DH) of the soluble collagen peptide solution was 79%.

The soluble collagen supernatant was passed through a 1 kDa cut-off membrane to separate it into <1 kDa and >1 kDa fractions. The latter was then passed through a 3 kDa membrane to produce 1-3 kDa and > 3 kDa fractions.

The collagen <1 kDa fraction accounted for 2% of the protein peptides in the liquor, the 1-3 kDa fraction for 22% and the >3 kDa fraction for 62%. As with the 1-3 kDa BW preparation, the Collagen 1-3 kDa fraction was bacteriostatic against the tested Gram-positive bacteria at a concentration of 4 mg/mL but bactericidal against the Gram-negative bacteria.

In kit assays, the IC_{50} values for ACE and DPP4 inhibition for the Collagen 1-3 kDa fraction were 270 µg/mL (1.85 U/mg) and 100 µg/mL (5.0 U/mg), respectively.

In a preliminary study, the Collagen 1-3 kDa fraction was found to be the most potent of the ultrafiltrated fractions in promoting wound healing in vitro. After fractionation by flash

 doi:10.20944/preprints202509.1539.v1

chromatography (Figure 6), three peaks (1, 2, and 3) were recovered and freeze-dried for further analysis.

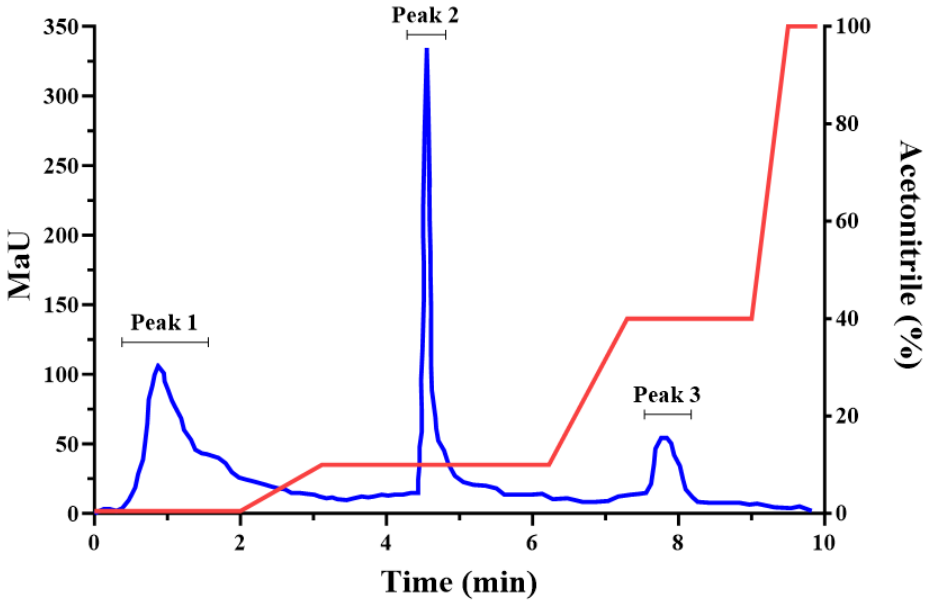

Figure 6. Graphic representation of separation of the *I. badionotus* Collagen 1-3 kDa fraction by flash chromatography. Data was acquired from the original printout (Supplementary Figure 1) with Plotdigitizer, and drawn with GraphPad Prism.

Before use in the scratch wound assay, the Collagen 1-3 kDa and Peak 2 fractions were tested for cytotoxicity by the standard MTT method. No toxicity was evident when cells were mixed with the fractions at a concentration of 0.2 mg/mL. This concentration was therefore used in the subsequent wound-healing assay.

2.3.7. Wound-healing assay

The peptide fractions of *I. badionotus* collagen were tested for potency of wound healing in a scratch assay model with human keratinocyte (HaCat) cells in culture medium containing 10% foetal calf serum (Figure 7). Collagen 1-3 kDa and Collagen 1-3 kDa Peak 2 (Figure 6) both promoted wound healing (Figure 7a and 7b), while collagen <1 kDa and collagen >3 kDa (Figure 6) exhibited little or no activity. Collagen 1-3 kDa Peak 2 had the highest activity (Figure 7).

Similar wound closure trends were observed when these fractions were tested in another laboratory. However, closure rates were slower, possibly because of the much lower levels of foetal calf serum (1%) in the culture medium (Supplemental Fig. 2).

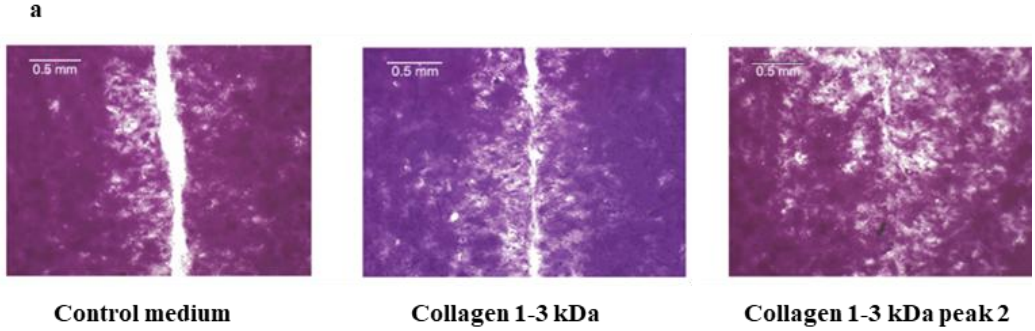

 doi:10.20944/preprints202509.1539.v1

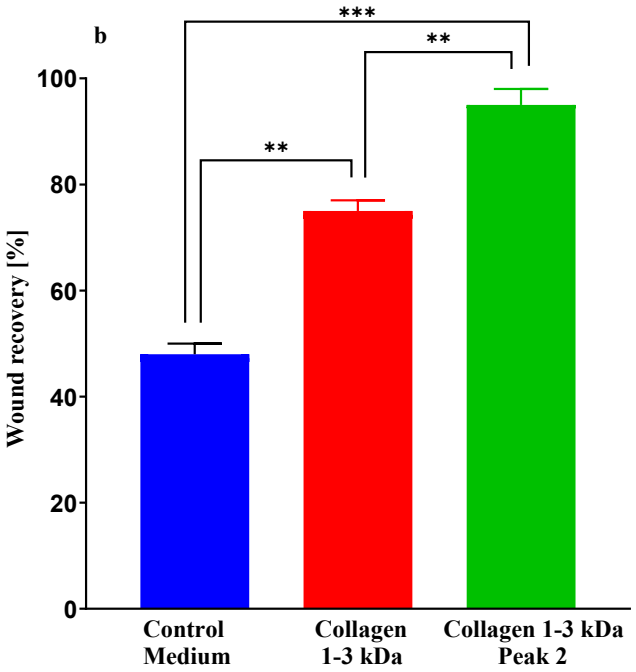

Figure 7. Images (a) and evaluations (b) of wound healing in a scratch assay based on human keratinocytes cultured for 24 h in media containing 10% foetal calf serum with or without ultrafiltrate fractions of digested collagen from *I. badionotus* (Collagen 1-3 kDa) or a further purified preparation (Collagen 1-3 kDa Peak 2). Marked values differ significantly (** $p \leq 0.01$; *** $p \leq 0.01$).

2.3.8. Gene expression analysis

Relative expression of *IL1α*, *IL6*, *TGFβ1*, *DSG1*, *DSG3* and *S100A7* genes in human keratinocytes collected from the wound healing assays after 24 h culture with *I. badionotus* preparations varied according to the individual fractions (Figure 8). When wounds were treated with 1-3 kDa BW, relative expression levels of *IL1α*, *IL6*, and *TGFβ1* were significantly lowered (below one time-fold) compared to those in the control media, but *S100A7* was significantly elevated. Only *IL1α* and *DSG1* expression was reduced when wounds were treated with Collagen 1-3 kDa. This fraction increased *S100A7* expression, but to a lesser extent than with 1-3 kDa BW. In contrast, treatment with Collagen 1-3 kDa Peak 2 elevated expression of *IL1α* and *IL6*, but did not affect *S100A7* or other genes.

 doi:10.20944/preprints202509.1539.v1

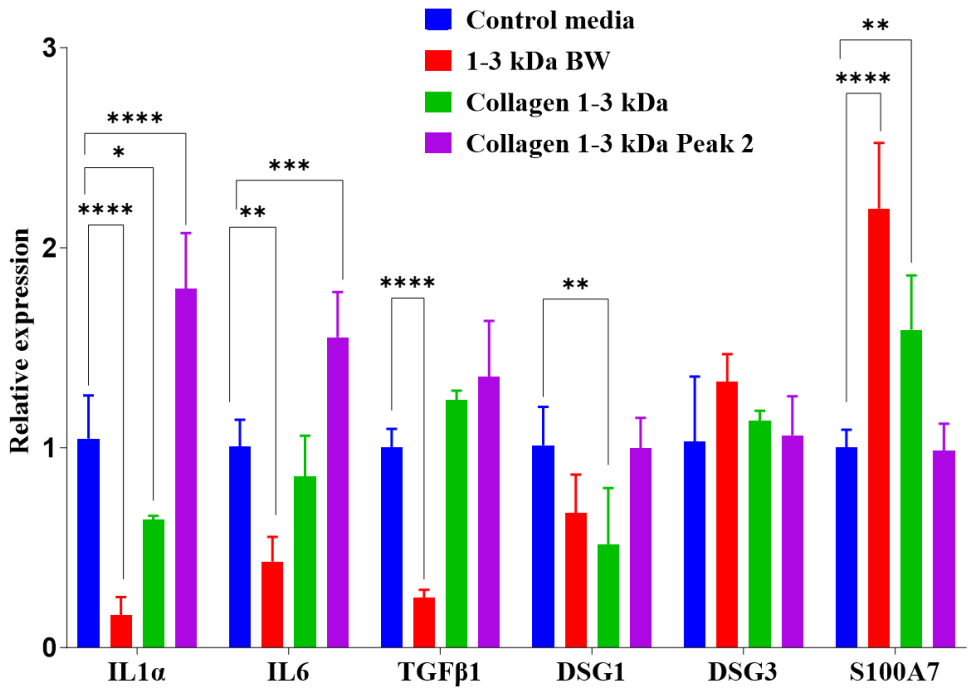

Figure 8. Expression of *IL1α*, *IL6*, *TGFβ1*, *DSG1*, *DSG3* and *S100A7* in human keratinocytes recovered from the wound-healing assay after culture [10% foetal calf serum] for 24 h with 1-3 kDa BW, Collagen 1-3 kDa or Collagen 1-3 kDa Peak 2. * $p \leq 0.05$, ** $p \leq 0.01$, *** $p \leq 0.001$, **** $p \leq 0.0001$.

2.3.9. Antioxidant activities of collagen fractions

Previous studies have suggested an association between the antioxidant capacity of collagen peptides and their potential to promote wound healing. So, these activities were determined using the ABTS and ORAC methods (Figure 9). Fractions (<1 kDa, 1-3 kDa and >3 kDa) of *I. badionotus* collagen were each active in both assays, but the Trolox equivalent levels were by far the highest with Collagen 1-3 kDa. Collagen 1-3 kDa Peak 2, obtained by flash chromatography, also had potent antioxidant activities. However, the balance between the activities changed. The Trolox equivalent levels in the ORAC assay for Collagen 1-3 kDa Peak 2 were significantly higher than in Collagen 1-3 kDa, from which it was derived, while ABTS assay values were unaltered. Indeed, the ORAC-ABTS ratio for Collagen 1-3 kDa Peak 2 resembled that for 1-3 kDa BW (Figure 1).

 doi:10.20944/preprints202509.1539.v1

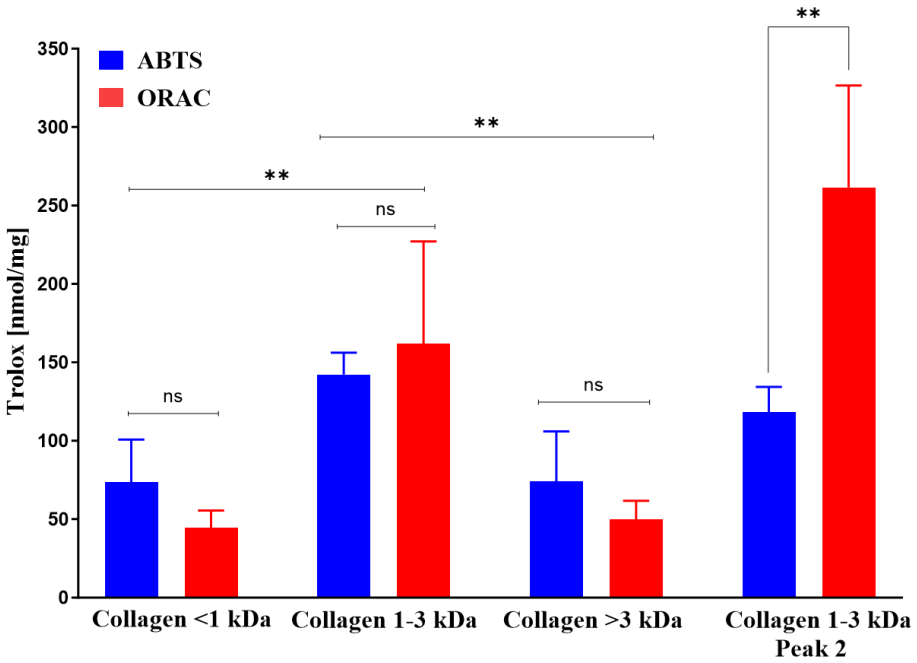

Figure 9. The constituent antioxidant activities (ABTS and ORAC) of ultrafiltrate fractions of digested collagen from *I. badionotus* or Collagen 1-3 kDa Peak 2. Values with ** differ significantly ($p \leq 0.01$).

3. Discussion

The primary purposes of this research were to isolate and characterize the collagen of *I. badionotus* and evaluate whether peptide fractions derived from it could promote wound healing and closure in a scratch wound model based on keratinocytes (HaCaT cells) in culture [16,17]. The present study is, as far as we can ascertain, the first to demonstrate that low-molecular-weight peptides of collagen from skin-free *I. badionotus* body wall promote wound healing and closure in vitro.

Proximal analysis of *I. badionotus* harvested for the present study off the coast of Telchac Puerto, Yucatan, Mexico, was generally like that of *I. badionotus* collected off Dzilam de Bravo, Yucatan, Mexico [18], and off the Caribbean coast of Colombia at Santa Marta [19]. Its composition was also similar to the general ranges expected for other commercial sea cucumber species captured worldwide [6,20–26].

Sea cucumbers are rich sources of bioactive factors, including peptides [native and proteolytic digestion products] that can promote wound healing in vitro and in vivo [7,8,29,30]. The levels and potency of these individual bioactive components vary significantly depending on the species, growth environment, season, body composition, and the handling or processing of captured or harvested animals [9–11].

While some bioactive properties of derivatives from *I. badionotus* from Yucatan have previously been evaluated in vitro and in vivo [14,15,31], their wound-healing capacity has not. The remedial efficacy of these derivatives was generally similar to that reported for other commercially-important sea cucumber species [7,8,32]. As with other species, the wound-healing bioactivity of *I. badionotus* was mainly associated with a low-molecular-weight fraction of the body wall digest [7,29], specifically one of 1-3 kDa. Again, as with other species, the body wall fraction of *I. badionotus* had significant antioxidant, inhibitory and antibacterial activities [33–35].

Collagen is the major individual protein in sea cucumber body wall. However, content can vary between 20% and 70% of total protein depending on species, growth environment, and final body weight [36,37]. The collagen content of *I. badionotus* from Yucatan was approximately 50% of the dry body wall, and thus similar to levels reported in most commercially-harvested species [18,36,37].

The collagen isolated from *I. badionotus* body wall was type I, which mainly consists of multiple $\alpha 1$ and $\alpha 2$ subunits [38]. The SDS-PAGE profile was similar to that for collagen from *Stichopus*

 doi:10.20944/preprints202509.1539.v1

horrens, *Holothuria scabra*, and *H. leucospilota* [39]. The amino acid composition, SEM, UV-spectrum, FTIR spectroscopy, and CD studies confirmed its substantive similarity - though not complete identity - to collagens from other sea cucumber and marine species [39–44]. The denaturation temperature (Td) of *I. badionotus* collagen [32.5 °C] was in the high range for sea cucumber collagens and thus similar to those from *S. horrens* [32.8 °C], *H. scabra* [32.3 °C], and *H. leucospilota* [34.6 °C] [39]. But, the Td was much higher than for collagens from *Stichopus monotuberculatus* [30.2 °C] [45] *Parastichopus californicus* [18.5 °C] and others [20,46]. The high Td value for *I. badionotus* collagen will, at least in part, be due to its elevated imino acids content (Hyp and Pro); these play a critical role in steadying the triple helix structure of collagen and enhancing its thermal stability [38,47]. Overall, *I. badionotus* collagen composition and organization were similar to that of other sea cucumber collagens, though with some unique structural and reactive features.

In the present study, the 1-3 kDa fraction of *I. badionotus* body wall (1-3 kDa BW), the Collagen 1-3 kDa component, and the Collagen 1-3 kDa Peak 2 fraction each promoted wound healing and closure in the scratch wound assay with keratinocyte (HaCat) cells in culture. These findings are consistent with reports on the wound-healing properties of other sea cucumber species derivatives [8,29,32,48]. Collagen 1-3 kDa Peak 2 was the most potent (95% closure in 24 hours), while Collagen 1-3 kDa, from which it was derived, was less efficient (78% closure in 24 hours). The 1-3 kDa BW fraction was almost as good as the Collagen 1-3 kDa Peak 2 (90% closure in 24 hours).

Restitution in vitro or in vivo involves a multiplicity of cellular responses and changes which allow keratinocytes on the borders of a wound in a cell layer to proliferate and migrate to fill and close the gap. These events include a transient reduction in cell-cell interactions and partial release, allowing cells to spread and migrate across the wound, followed by repolarisation and maturation as the wound is covered and healing is completed [49,50]. Such processes are strictly regulated by growth factors, hormones and cytokines, derived locally or from cells [51] underlying or associated with the disrupted layer [16,17,52–56].

Once a wound is made in a keratinocyte cell layer, all the restitution processes activate in a coordinated manner. However, exposure to external factors may enhance or disrupt individual or multiple aspects of the cellular repair sequence [16,52,57–63].

Interleukin 1α (*IL1*α), Interleukin 6 (*IL6*), Transforming growth factor beta (*TGF*β), Desmoglein-1 (*DSG1*), Desmoglein-3 (*DSG3*) and S100 calcium-binding protein A7 or psoriasin (*S100A7*) have important roles in various aspects of wound healing by HaCat (keratinocyte) cells. Their expression levels vary with time in untreated wounds according to the healing stage and key repair processes being carried out [16,52,54,56]. The expression and timing of these genes can be influenced by external conditions that alter the efficacy and integrity of the repair process.

Many studies have demonstrated that antioxidants from natural sources, including small peptides of marine collagens, facilitate wound healing in vitro and in vivo, probably by moderating and quenching excessive oxidative stresses that can occur during key stages of natural repair and severely limit their efficacy [64–67]. Data from the present study suggest a positive correlation between the antioxidant activities, in particular peroxyl radical neutralising actions[68,69], of the tested peptide preparations and their efficacy in wound healing. However, the marked differences in gene expression at 24 hours, associated with wound healing mediated by each tested sea cucumber fraction, suggest that the antioxidant activity protected and facilitated repair, but is merely one of the factors involved.

The purified Collagen 1-3 kDa Peak 2 peptide fraction, the most potent promoter of wound healing, was associated with slightly elevated expression of *IL-1*α and *IL-6* at 24 hours. High expression of these pro-inflammatory factor levels is to be expected and is important for jump-starting wound repair; their levels usually fall below or near to control cell levels as wound closure or near-closure occurs [16,52,54,56–58,61]. The present finding is thus unexpected. However, given the important involvement of *IL1*α and *IL6* in driving wound healing, one possible reason that wound healing driven by Collagen 1-3 kDa Peak 2 peptides is highly effective is that it occurs within an environment of persistent low-grade inflammation. Whether this pro-inflammatory signal resolves

 doi:10.20944/preprints202509.1539.v1

appropriately at full wound closure or leads to a prolonged inflammatory state at later time points is a critical question for future studies.

The exact mode of action of collagen peptides in wound repair in keratinocytes remains unclear. However, wound healing is mediated through cellular receptors for growth factors, such as those for epidermal growth factor (EGF), transforming growth factor-α (TGFα), and keratinocyte growth factor (KGF) [62,63] and an array of immune-pathway and cytokine-initiating receptors [70–72]. In many cases, simultaneous activation of two or more of these receptors in combination leads to better or more effective wound repair than activation of single receptors alone [62,63]. Previous studies have shown that some collagen peptides can act as receptor agonists, thereby activating key cellular receptors and associated cellular signalling pathways to modulate metabolism and cell proliferation [70–73]. Their actions are usually beneficial but can be detrimental [72].

In the present study, sea cucumber Collagen 1-3 kDa Peak 2 peptides promoted wound healing over 24 hours in vitro. However, the gene expression profile suggests their important roles are in the activation or amplification of the early inflammatory phase of tissue repair, with lesser effects on the later stages of repair.

In contrast, the original collagen digest (Collagen 1-3 kDa) preparation, from which Collagen 1-3 kDa Peak 2 was derived, induced a slower rate of wound healing, but one in which the gene expression profile at 24 hours - including elevated *S100A7*, a marker of antimicrobial defence and epithelial differentiation - had strong similarities to those observed during wound repair in HaCat cells treated with various short- or long-term non-direct repair-promoting measures [16,52,54,56–58,61]. The Collagen 1-3 kDa preparation appeared to have broader actions over the integrated repair process than its more highly purified counterpart. On balance, this preparation may favour the boosting of cellular movement and protection, as well as strengthening of the barrier following initial inflammation-driven responses.

The Collagen 1-3 kDa fraction contains many more collagen-derived peptides than its highly purified counterpart, Collagen 1-3 kDa Peak 2. These additional peptides may inhibit, or compete or interfere with the actions of the most potent promoters of wound healing, thereby, as observed with Collagen 1-3 kDa, slowing the rate of repair. However, since collagen peptides can also act on a broad array of cellular receptors [62,63,72], some of these additional peptides may also bind to and activate different receptors and cell-signalling pathways that facilitate coordinated and efficient wound repair.

The low-molecular-weight preparation from digested sea cucumber body wall (1-3 kDa BW) promoted more rapid repair than did the Collagen 1-3 kDa peptides and was almost as effective as the Collagen 1-3 kDa Peak 2. The gene expression profile it elicited was like that in HaCat cells when wound healing is induced by various short- or long-term non-targeted treatments [16,52,54,56–58,61]. Indeed, it was closest to that expected during unstimulated repair. This finding suggests that 1-3 kDa BW may act predominantly as a stimulus for cellular expansion, movement, and protection, accompanied by an attenuation of the initial actions of inflammatory signalling.

Sea cucumber whole-body wall contains many proteins unrelated to collagen, as well as other bioactive factors that may facilitate wound repair [8,14,29,74]. Fragments of these proteins or small molecular weight bioactive factors may act in synergy with the collagen peptides in the 1-3 kDa BW fraction to better modulate/integrate wound healing. These aspects of integrated wound repair induced by the 1-3 kDa BW fraction of *I. badionotus* require further study.

Taken together, these results indicate that the three sea cucumber peptide preparations examined in this study all promoted wound healing in vitro, but did so by acting on repair processes in different ways: the highly purified Collagen 1-3 kDa Peak 2 may act primarily via early inflammatory response-driven mechanisms, Collagen 1-3 kDa may favour cellular movement/protection and epithelial barrier reinforcement processes, while the 1-3 kDa BW fraction of digested body wall may act through resolution of inflammation and facilitation of cell movement/protection and maturation of cells at closure.

 doi:10.20944/preprints202509.1539.v1

4. Materials and Methods

4.1. Materials and Reagents

Porcine stomach mucosa pepsin (EC3.4.23.1), dialysis membrane (14 kDa MWCO), and calf skin type I collagen standard solutions were purchased from Sigma-Aldrich (St. Louis, MO, USA); *Carica papaya* papain (30,000 U/mg; E.C. 3.4.22.2) and ultrafiltration membranes (1 and 3 kDa MWCO) from Merck Corporation (Burlington, MA, USA), and solvents for amino acid analysis were HPLC-grade from T.J. Baker Chemicals (Baker, PA, USA). All other chemicals were analytical grade.

4.2. Collection and Processing of Sea Cucumber

Wild sea cucumber *I. badionotus* was collected manually from the seafloor by scuba diving (approximately 10 metres depth). They were collected off the coast of Telchac Puerto, Yucatan, Mexico, under collection permit PPF/DGOPA-0126/15 issued by the National Commission for Fisheries and Aquaculture (CONAPESCA). To prevent proteolysis or autolysis of the organisms due to sudden temperature changes, they were placed in individual, seawater-filled plastic bags at collection depth. When brought to the surface, they were placed in seawater coolers at approximately the same temperature (22 to 24 °C) as the collection depth. They were transported to the Telchac Puerto marine station of the Centro de Investigación y Estudios Avanzados del Instituto Politécnico Nacional (CINVESTAV-IPN), where they were kept under controlled (23 - 24 °C) conditions until processed in the Aquaculture Nutrition Laboratory at the CINVESTAV Merida campus.

4.3. Proximate Composition

For proximal analysis, some animals were removed from the holding tank and washed with cold distilled water to remove excess salt and sediment [31]. After a longitudinal ventral incision, the internal organs were removed from within the body wall, the ends of the body cut off, the remainder of the body cut longitudinally and frozen in liquid nitrogen for transport to the laboratory in Merida. In the laboratory, the samples were partially freeze-dried (10 h), the skin removed, the body wall cut into squares and dried by lyophilization.

The moisture and ash contents of samples of whole-body wall were determined following standard AOAC methods [15,31]; a portion of tissue was dried in an oven at 105 °C for 24 h to measure moisture content, and another was reduced in a muffle furnace at 550 °C for 6 h to measure ash content. Lipid content was estimated by the Folch method [15,31]. Nitrogen content was measured with an elemental analyzer (FLASH 2000, ThermoScientific, Waltham, MA, USA), and protein content calculated by multiplying by the factor 6.25.

4.4. Skin-Free Body Wall Digest

Twenty grams of dry, skin-free body wall was washed twice with sterile cold water and incubated overnight in a water bath at 60 °C with 200 mL sodium acetate pH 6 buffer (50 mM sodium acetate, 50 mM L-cysteine and 5 mM EDTA) containing 2 grams papain. The enzyme was deactivated by heating the liquor at 80 °C for 10 min and then cooled. The resulting liquor was first filtered through glass wool and then centrifuged at 10,000 × *g*. The supernatant was recovered and sequentially ultrafiltered using an Amicon® Stirred Cell (Merck) and ultrafiltration membranes with 1 kDa and 3 kDa cut-offs. The liquor was first passed through a 1 kDa cut-off membrane to obtain a >1 kDa retentate fraction and a <1 kDa permeate fraction. The >1 kDa retentate was then passed through a 3 kDa cut-off membrane to obtain 1-3 kDa and >3 kDa fractions.

4.5. Pepsin-Soluble Collagen Extraction

Collagen from the skin-free body wall was extracted according to the method of Liu et al. [46], with slight modifications. All processing was done at 4 °C.

 doi:10.20944/preprints202509.1539.v1

Fifty grams of dry, skin-free body wall were washed in one litre of cold deionized water under gentle agitation for 1 hour (changed at 30 min). The water was replaced by the same volume of an ethylenediamine-tetra-acetic (EDTA) solution [4 mM in Tris-HCl (0.1 M, pH 8.0)] and stirred continuously (500 rpm at 4 °C) for 48 h with two changes per day. The remaining tissue pieces were recovered by sieving through cheesecloth and washing with cold deionized water until effluent pH reached approximately neutral. The resulting precipitate was dispersed in 20 volumes (w/v) NaOH (0.1 M) and stirred for two days (500 rpm at 4 °C) to dissolve the non-collagenous components. The collagen fibres were recovered by gentle sieving and washing several times with cold deionized water until reaching a pH near neutral. They were dispersed in 0.5 M acetic acid containing 2% (w/w) pepsin and incubated for 72 h. The solubilized collagen fibres were salted out from the solution by adding NaCl to make it 1.2 M with respect to the salt and leaving the suspension for two days at 4 °C, followed by centrifugation at 15000 x g for 15 min. The resultant pellets were resuspended in acetic acid solution (0.1 M) and dialyzed (12,000 – 14,000 kDa membrane) in Na_2HPO_4 phosphate buffer (0.02 M, pH 8.0) for 48 h, with a solution change every 12 h. The purified collagen was freeze-dried and stored at 4 °C until use.

4.6. Collagen characterization

4.6.1. Electrophoresis

Sodium dodecyl sulfate-polyacrylamide gel electrophoresis (SDS-PAGE) analysis was performed according to the Laemmli method [75,76]. The lyophilized collagen was dissolved in 0.1 M acetic acid (final protein concentration, 4 mg mL^{-1}) and then mixed at a 1:2 (v/v) ratio with the sample buffer (0.5 M Tris-HCl, pH 6.8, containing 5% SDS, 20% glycerol, 5% β-ME and 0.2% bromophenol blue). The mixed solution was incubated at 95 °C for 5 min and then subjected to electrophoresis (7.5% separator and 4% stacking gels) using a Mini-PROTEAN 3 Cell (Bio-Rad Laboratories, Hercules, CA, USA). After electrophoresis, samples were viewed by staining with Coomassie brilliant blue and destained in 40% methanol and 10% acetic acid. A molecular weight protein marker (Precision Plus Protein Standards All Blue, Bio-Rad) was used to estimate collagen molecular weight.

4.6.2. Amino acid composition

Lyophilized collagen was analyzed for amino acid composition according to the PicoTag procedure (Waters, USA). Samples were hydrolyzed with 6 N HCl with 0.1% phenol and incubated in a nitrogen atmosphere at 110 °C for 22 h. After hydrolysis, samples and standards were derivatized with phenyl isothiocyanate (PITC) reagent and reconstituted in a sodium phosphate buffer (5 mM, pH 7.4) containing 5% (v/v) acetonitrile. The derivatives were analyzed by reverse phase chromatography (RP-UHPLC) in an Ultimate 3000 HPLC system (ThermoScientific, Waltham, MA, USA). Amino acid quantification was done using a standard amino acid mixture as reference and expressed as the number of residues per 1000 total residues.

4.6.3. X-ray Diffraction (XRD) and Circular Dichroism (CD)

Collagen crystal structures were studied using an x-ray diffraction instrument (Bruker D8 Advance DaVinci, DE) under these conditions: Cu Ka source, 40 kV tube voltage, 40 mA tube current, 3-60° scanning range (2θ), and 0.02°/s scanning speed. Secondary structure preservation of the collagen was assessed by Far-UV CD using a Chirascan spectropolarimeter (Applied Photophysics Ltd., Leatherhead, UK). The lyophilized collagen was dissolved in 0.1 M acetic acid at 0.1 mg mL^{-1} and continuously stirred at 4 °C for 24 h. Collagen solutions were placed in a quartz cell with a 0.1 cm path length. CD spectra were recorded in a 185-260 nm range at 4 °C, a 50 nm/min scan speed, and a 0.1 nm interval. Denaturation temperature (Td) was calculated from the ellipticity value at a fixed wavelength of 222 nm in the 4 - 65 °C range at a 1 °C/min rate.

 doi:10.20944/preprints202509.1539.v1

4.6.4. UV-VIS and Fourier Transform Infrared (FTIR) Spectra

The collagen UV spectra were obtained using a Multiskan GO spectrophotometer (Thermo Fisher Scientific, USA). Lyophilized collagen was dissolved in acetic acid at a 0.1 mg mL^{-1} concentration and continuously stirred at 4 °C for 12 h. The sample solution was placed in a quartz cell with a 10 mm path length. The spectra were recorded at 25 °C at a 1 nm interval in the 200 - 400 nm range. FITR spectra were recorded with a Nicolet iS5 (Thermo Scientific , Mexico) spectrophotometer using the ATR methodology. Lyophilized collagen was clamped onto the zinc selenide diamond crystal, and its spectra recorded with a spectrometer at 2 cm^{-1} resolution in the 400 - 4000 cm^{-1} range. The baseline was set with 0.1 M acetic acid.

4.7. Collagen Hydrolysate Preparation

Hydrolysis of collagen was done with papain, according to Chotphruethipong et al. [77] and Vieira and Murao [78]. Ten grams of collagen were suspended in 100 mL acetate buffer (pH 6) and digested with papain (enzyme:substrate ratio, 1:10, w/w) for 12 h at 60 °C. The solution was heated at 80 °C for 5 min to inactivate the enzymatic reaction, filtered through glass wool and centrifuged at 5000 × g for 30 min at 4 °C to obtain a clear supernatant. The resulting soluble collagen peptide solution was freeze-dried. Its degree of hydrolysis (DH) was measured by spectrophotometry following Nielsen et al. [79], using NAC (N-Acetyl-L-cysteine) as a thiol reagent, as described by Spellman et al. [80]; the DH was 79%.

4.7.1. Ultrafiltration

Fractionation of the soluble collagen peptide solution was conducted as per section 4.4, resulting in three fractions: Collagen < 1 kDa, Collagen 1-3 kDa, and Collagen > 3 kDa.

4.7.2. Flash Chromatography of Collagen 1-3 kDa

The 1-3 kDa isolate was reconstituted in deionized water (40 mg mL^{-1}), loaded onto a SNAP Ultra C18 column (Biotage® HP-Sphere) and stepwise eluted with water:acetonitrile (gradient of 0% to 40% acetonitrile), at a 25 mL/min flow rate, and 215 and 280 nm wavelengths. Fractions (5 mL) were collected, pooled in accordance with the graphic profile and lyophilized. Data was recovered from the printout using Plotdigitizer (https://plotdigitizer.com) and printed out using GraphPad Prism (https://www.graphpad.com).

4.7.3. Antioxidant activity

4.7.3.1. ABTS+ Scavenging Activity

Scavenging antioxidant activity was measured by the 2,2-azinobis[3-ethylbenzothiazoline-6-sulfonic acid] (ABTS+) method [81]. Briefly, the radical ABTS+ stock solution was generated by mixing (v/v) 7 mM ABTS and 2.45 mM potassium persulfate in the dark at room temperature for approximately 16 h. The ABTS+ working solution was produced by diluting the stock solution in 5 mM sodium phosphate buffer (pH 7.4) at 734 nm absorbance and a 0.70 ± 0.02 range. Working solution (180 µL) was added to 20 µL peptide fraction sample or the standard 6-hydroxy-2,5,7,8-tetramethylchroman-2-carboxylic acid; Trolox) in PBS. Absorbance was measured after 6 min in a spectrophotometer (Multiskan Go, ThermoScientific, Waltham, MA, USA). Samples were analyzed in three replicates. Percentage inhibition was calculated and plotted as a function of the amount of antioxidants (mg) or standard (µmol Trolox), and Trolox equivalent antioxidant capacity values calculated.

4.7.3.2. Oxygen Radical Absorbance Capacity (ORAC)

The ORAC assay was conducted per Garret et al. [82]. Samples and standards were prepared in PBS (1 mg mL^{-1}, double diluted and 20 µl of each dilution placed in the wells of a 96-well plate. Two

 doi:10.20944/preprints202509.1539.v1

hundred microlitres fluorescein (3, 6-dihydroxyspiro [isobenzofuran-1[3H],9[9H]-xanthen]-3-one) [FL] stock (30 nmol L^{-1}) and 75 µl 2, 2-azobis (2- amidinopropane) dihydrochloride [AAPH]) stock (12 mmol L^{-1}) were added to each well. A standard curve was produced using an antioxidant calibrator (Trolox, 0–5 nmol L^{-1}). The reaction was conducted at 37 °C, and fluorescence recorded every 3.5 min for 31 cycles in an Apliskan plate reader (ThermoScientific, Waltham, MA, USA) at 485 nm excitation and 520 nm emission. Three replicates were done for each sample and standard. ORAC values were expressed as µmol Trolox equivalents (TE)/mg sample.

4.7.3.3. Further Analyses

Cytotoxicity of the 1-3 kDa BW, Collagen 1-3 kDa and Collagen 1-3 kDa Peak 2 preparations was evaluated by the thiazolyl blue tetrazolium bromide (MTT) assay with keratinocyte (HaCat) cells, according to Mani & Swargiary [83]. The concentrations used in the assay were 0.5, 0.25, 0.125, 0.0625 and 0.0031 mg/mL. Angiotensin I-converting enzyme (ACE) and dipeptidyl peptidase 4 inhibitory activities were quantified using assay kits (C50002 and Mak088, Sigma-Aldrich). Both were done in triplicate according to the corresponding manufacturer protocol.

The antibacterial activity of *I. badionotus* peptide fractions was evaluated by culture of *Escherichia coli* ATCC 25922, *Pseudomonas aeruginosa* ATCC 13637, *Pseudomonas aeruginosa* 64D (MDR), *Staphylococcus aureus* ATCC 25725, *Staphylococcus aureus* MR (Methicillin resistant), *Enterococcus faecalis* ATCC 51299 (Vancomycin resistant) or *Enterococcus faecium* 683D (Vancomycin resistant) in Mueller-Hinton medium [$5x10^5$ cfu/mL], with or without extract, at six concentrations: 0.125mg/mL, 0.25mg/mL, 0.5mg/mL, 1 mg/mL, 2 mg/mL, and 4 mg/mL. After overnight incubation at 37 °C for 18 h, 10 µL of these mixtures were plated on Blood agar or Luria Bertani agar and incubated for a further 18 h at 37 °C.

4.8. Wound healing In Vitro

4.8.1. Scratch Wound Healing Assay

Primary stocks of immortalized human keratinocytes (HaCat) cell line provided by Dr. Oscar Medina Contreras (Hospital Infantil de Mexico "Federico Gómez", Mexico City) were cultured in DMEM/Ham's F12 medium supplemented with bicarbonate, an antibiotic-antimycotic, and 10% FBS (GIBCO), at pH 7.2 [57,84]. Cells were seeded on treated 75 cm^2 culture plates (NEST Scientific Inc., NJ, USA) and incubated at 37 °C in 5% CO_2. The culture medium was changed at three-day intervals.

The keratinocytes were harvested when 80% confluent. The medium was removed, the cell layer washed with PBS (pH 7.2), 3 ml trypsin-EDTA [Trypsin 0.05% – EDTA 0.53 mM] added to the plate, and the plate incubated at 37 °C for 4 mins to detach the cells. Five ml culture medium were added to the plate, the total volume recovered and placed in a 15 ml centrifuge tube. After centrifugation at 1500 rpm for 5 minutes, the supernatant was removed and 1 mL culture medium added. The tube was mixed gently to disperse the cells, and counts done using a manual hemocytometer. The cell preparation was then diluted with medium to a 160,000 cells/ml concentration.

For the assay, 300 µl medium containing 50,000 keratinocytes were added to each well of a 48-well plate (NEST Scientific Inc., NJ, USA), and the plate incubated at 37 °C in 5% CO_2. Cell growth was monitored until 80% confluence was attained. The culture medium was then removed from each well, and the adherent cells washed twice with 500 µl fresh, sterile PBS 7.2. During the second wash, a scratch wound was made in the cell layer using a one-ml pipette (blue) tip. The PBS pH 7.2 was removed, and a third wash done.

Pre-prepared collagen peptide fractions (60 µg in 0.3 mL) or control medium (0.3 mL) were added to the appropriate wells [six replicates each], and the plates incubated at 37 °C and 5% CO_2. The healing process was monitored by taking images at 0 and 24 hours post wound induction via an inverted, phase-contrast microscope (10X). Wound healing rate was assessed using the ImageJ software (Gebäck, Zurich, Switzerland). Means and standard deviations were calculated, and

 doi:10.20944/preprints202509.1539.v1

statistical significance evaluated by multiple comparisons and post-hoc significance tests using the GraphPad software.

4.8.2. Gene expression

Expression of several genes involved in the healing process was quantified (Table 2), using the beta actin gene (*β-actin*) as a housekeeping gene.

Table 2. Primer sequences used for real-time quantitative PCR.

Target gene	Forward 5′ - 3′ Reverse 3′ - 5′	Reference
ILlα	F: CGCCAATGACTCAGAGGAAGA R: AGGGCGTCATTCAGGATGAA	Wiegand et al, 2021 [52]
IL6	F: AGACAGCCACTCACCTCTTCAG R: TTCTGCCAGTGCCTCTTTGCTG	NM_000600.5
TGFβ1	F: GAGCCCTGGATACCAACTATT R: AGGACCTTGCTGTACTGTGTG	Wallace et al., 2023 [85]
DDSG1	F: TCCCCACATTTCGGCACTAC R: GCCCAGAGGATCGAGAATAGG	Wiegand et al, 2021 [52]
DSG3	F: GTCAGAACAATCGGTGTGAGATG R: TGCGGCCTGCCATACCT	Wiegand et al, 2021 [52]
SI00A7	F: GTCCAAACACACACATCTCACT R: TCATCATCGTCAGCAGGCTT	Wiegand et al, 2021 [52]
β-actin	F: GATCATTGCTCCTCCTGAGC R: GTCATAGTCCGCCTAGAAGCAT	NM_001101.5

RNA extraction from human keratinocyte (HaCat) cells was done using a commercial Animal Tissue RNA Purification kit (Norgen Biotek Corp©), following manufacturer protocol. Extracted RNA concentration and purity were assessed using a Thermo Scientific NanoDrop™ 2000c spectrophotometer (Thermo Fisher Scientific., Waltham, MA, USA). The extracted RNA samples were standardized to a 100 ng/µL final concentration, from which the cDNA of all samples was prepared using the commercial High-Capacity cDNA Reverse Transcription Kit (Thermo Fisher Scientific™), following manufacturer protocol. Primer calibration curves were generated using five serial dilutions at a 1:5 dilution factor

Quantification of gene expression was done by real-time quantitative PCR (qPCR) on a Rotor-Gene Q thermal cycler (QIAGEN®), using the commercial Maxima SYBR Green/ROX qPCR Master Mix/2X kit (Thermo Fisher Scientific™). Reaction mixes were standardized into a final volume of 15 µL containing 7.5 µL Maxima SYBR Green 2X reagent (QIAGEN), 1 µL diluted cDNA (5 µL cDNA + 20 µL water), 0.5 µL of each primer (5 µM), and 5.5 µL nuclease-free water. Amplification thermal cycling conditions were: initial denaturation at 95 °C for 10 minutes; 35 cycles denaturation at 95 °C for 10 seconds; an extension at 60 °C for 45 seconds. Amplification specificity was corroborated by analysis of the dissociation curve of the formed products. The results were processed with the Rotor-Gene software version 6.1.

Evaluation of gene expression was done by evaluating three replicates of each sample from the 24 h scratch wound assay. The quantifications were based on the threshold cycle (Ct) value and the Ct values for each replicate. Changes in relative gene expression were calculated using the delta delta Ct (ΔΔCt) relative quantification method [86–89].

4.9. Statistical analysis

 doi:10.20944/preprints202509.1539.v1

GraphPadPrism (https://www.graphpad.com/) was used to conduct multiple-comparison statistical analysis, and the appropriate post-hoc tests run to evaluate statistical significance.

5. Conclusions

The body wall of *I. badionotus* from the Yucatan Peninsula contained collagen levels comparable to those in other commercially-harvested sea cucumber species. Collagen composition and structure were like, but not identical to, other sea cucumber collagens. Ultrafiltered digests (1-3 kDa) of the collagen and further purified samples from the Collagen 1-3 kDa preparation, as well as a 1-3 kDa digest of whole-body wall, had potent antioxidant activities (in particular, peroxyl radical neutralizing actions). They promoted rapid wound healing in a scratch assay using keratinocyte (HaCat) cells. However, expression of genes associated with wound repair differed significantly between cells treated with preparations of 1-3 kDa body wall, Collagen 1-3 kDa, or Collagen 1-3 kDa Peak 2. Thus, low-molecular-weight peptides of *I. badionotus* collagen promoted wound healing. However, their mechanisms of action and the possible involvement of other small compounds in modulating or amplifying their actions remain unclear and require further study.

Supplementary Materials: The following supporting information can be downloaded at: https://www.mdpi.com/article/doi/s1: Supplemental Figure 1. Separation of the *I. badionotus* Collagen 1-3 kDa fraction by flash chromatography (Original print out). Supplemental Figure 2. Evaluation of wound healing in a scratch assay based on human keratinocytes cultured in medium containing 1% foetal calf serum plus or minus Collagen 1-3 kDa or Collagen 1-3 kDa Peak 2 for 24 h and 48 h.

Author Contributions: Conceptualization, L.O-C. and G.G. ; methodology, L.O-C; G.J.M.P.; O.M-C; L.C-C; H.C-L.; S.R-M; A.C-C; F.S-C; D.A.F.V; J.V.C-R; J.U.N. and C.P-C. software, X.X.; validation, L.C-C; O.M.C. and L.O-C.; formal analysis, L.O-C; O.M-C; L.C-C; H.C-L.; D.A.F.V; investigation, L.O-C.; G.G.; resources, L.O-C; R.R-C; M.A.O-N; O.M-C; data curation, G.G. and L.O-C.; writing—original draft preparation, G.G. and L.O-C.; writing—review and editing, L.O-C.; G.G.; M.A.O-N;L.O-C; O.M-C; L.C-C; H.C-L.; S.R-M; A.C-C; F.S-C; D.A.F.V; J.V.C-R and J.U.N.; supervision, L.O-C.; project administration, R.R-C.; funding acquisition, R.R-C and L.O-C.). All authors have read and agreed to the published version of the manuscript.

Funding: Secretaría de Ciencia, Humanidades, Tecnología e Innovación (Secihti) (Formerly: CONACyT) basic science grant 013/221734CB-2 (I0017) "Actividad antiinflamatoria y cicatrizante del pepino de mar (*Isostichopus badionotus*) en un modelo murino: caracterización de la actividad farmacológica y los mecanismos moleculares involucrados" to R R-C.; National Laboratory of Nano Biomaterials (LANBIO) as part of the project FOMIX-Yucatán 2008-1081160,CONACYT LAB-2009-01-123913,292692,294643and 299083.

Institutional Review Board Statement: The capture of wild *I. badionotus* was done with the authorization, participation, and supervision of the National Fisheries Institute, Yucalpeten, Yucatan, Mexico (INAPESCA, CRIP-Yucalpeten). Sea cucumber handling and euthanasia was in accordance with the Mexican Official Standard for the Care and Use of Laboratory Animals (NOM-062-ZOO-1999) and the rules of the CINVESTAV Internal Committee for the Care and Use of Laboratory Animals.

Data Availability Statement: The original contributions presented in this study are included in the article/**supplementary materials**. Further inquiries can be directed to the corresponding author/s.

Acknowledgments: Thanks are due Isabel Velázquez UNAM for sample preparation for CD measurements. Thanks also to Juan Antonio Perez-Vega for technical assistance. For their invaluable technical assistance, we thank Victor Rejón-Moo, Santiago Gónzalez-Gómez and Daniel Aguilar-Treviño of CINVESTAV-Mérida. We would like to express our gratitude to the Laboratorio National de Nano y Biomateriales, CINVESTAV-Merida, for access to its electron microscopy, x-ray and FTIR infrastructure. Finally, special thanks to Teresa Colas-Marrufo (Laboratory of Ictiology, CINVESTAV-Mérida) for technical assistance and to John Lindsay-Edwards for editing and proof reading of the manuscript.

Conflicts of Interest: The authors declare no conflicts of interest.

Abbreviations

AAPH: 2,2-Azobis (2-amidinopropane) dihydrochloride
ABTS: 2,2-Azinobis[3-ethylbenzothiazoline-6-sulfonic acid]
ACE: Angiotensin I-converting enzyme

 doi:10.20944/preprints202509.1539.v1

B-actin: Beta actin
BW: Body wall
CD: Circular dichroism
CFU: Colony-forming units
CINVESTAV: Centro de Investigación y de Estudios Avanzados
CONAPESCA: Comisión Nacional de Pesca y Acuacultura
DGS1: Desmoglein-1
DGS3: Desmoglein-3
DH: Degree of hydrolysis
DPP4: Dipeptidyl Peptidase-4
EDTA: Ethylenediamine-tetra-acetic
EGF: epidermal growth factor
FBS: Foetal bovine serum
FL: fluorescein (3,6-dihydroxyspiro [isobenzofuran-1[3H],9[9H]-xanthen]-3-one)
FTIR: Fourier transform infrared
HaCat: keratinocyte
IC_{50}: Half-maximal inhibitory concentration
IL1α: Interleukin 1α
IL6: Interleukin 6
KGF: keratinocyte growth factor
MTT: thiazolyl blue tetrazolium bromide
NAC: N-Acetyl-L-cysteine
ORAC: Oxygen radical absorbance capacity
PBS: Phosphate-buffered saline
PITC: Phenyl isothiocyanate
qPCR: Quantitative polychrome chain reaction
RP-UHPLC: -ultra high pressure liquid chromatography
S100A7: S100 calcium-binding protein A7 or psoriasin
SDS-PAGE: Sodium dodecyl sulfate-polyacrylamide gel electrophoresis
SEM: Scanning electron microscope
TE: Trolox equivalents
TGFα: Transforming growth factor alpha
TGFβ1: Transforming growth factor beta one
XRD: X-ray diffraction

References

1. Mercier, A.; Gebruk, A.; Kremenetskaia, A.; Hamel, J.-F. An Overview of Taxonomic and Morphological Diversity in Sea Cucumbers (Holothuroidea: Echinodermata). In *The World of Sea Cucumbers*; Mercier, A., Hamel, J.-F., Suhrbier, A., Pearce, C., Eds.; Elsevier, 2024; pp. 3–15.
2. Mercier, A.; Purcell, S.W.; Montgomery, E.M.; Kinch, J.; Byrne, M.; Hamel, J.-F. Revered and Reviled: The Plight of the Vanishing Sea Cucumbers. *Ann Rev Mar Sci* 2025, *17*, 115–142, doi:10.1146/annurev-marine-032123-025441.
3. Pangestuti, R.; Arifin, Z. Medicinal and Health Benefit Effects of Functional Sea Cucumbers. *J Tradit Complement Med* 2018, *8*, 341–351, doi:10.1016/j.jtcme.2017.06.007.
4. Okada, A.; Udagawa, S.; Kohtsuka, H.; Hayashi, Y.; Miura, T. Gene-Expression Patterns during Regeneration of the Multi-Organ Complex after Evisceration in the Sea Cucumber Eupentacta Quinquesemita. *Front Mar Sci* 2024, *11*, doi:10.3389/fmars.2024.1346172.
5. Liu, R.; Ren, X.; Wang, J.; Chen, T.; Sun, X.; Lin, T.; Huang, J.; Guo, Z.; Luo, L.; Ren, C.; et al. Transcriptomic Analysis Reveals the Early Body Wall Regeneration Mechanism of the Sea Cucumber Holothuria Leucospilota after Artificially Induced Transverse Fission. *BMC Genomics* 2023, *24*, 766, doi:10.1186/s12864-023-09808-1.

6. Maskur, M.; Sayuti, M.; Widyasari, F.; Haryo Bimo Setiarto, R. Bioactive Compound and Functional Properties of Sea Cucumbers as Nutraceutical Products. *Reviews in Agricultural Science* 2024, *12*, 45–64, doi:10.7831/ras.12.0_45.
7. Shou, Y.; Feng, C.; Lu, Q.; Mao, X.; Huang, H.; Su, Z.; Guo, H.; Huang, Z. Research Progress on the Chemical Components and Biological Activities of Sea Cucumber Polypeptides. *Front Pharmacol* 2023, *14*, doi:10.3389/fphar.2023.1290175.
8. Liang, Q.; Ahmed, F.; Zhang, M.; Sperou, N.; Franco, C.M.M.; Feng, Q.; Zhang, W. In Vivo and Clinical Studies of Sea Cucumber-Derived Bioactives for Human Health and Nutrition From 2012-2021. *Front Mar Sci* 2022, *9*, doi:10.3389/fmars.2022.917857.
9. Das, A.; Hossain, A.; Dave, D. The Effect of Pre-Treatment and the Drying Method on the Nutritional and Bioactive Composition of Sea Cucumbers—A Review. *Applied Sciences* 2024, *14*, 6475, doi:10.3390/app14156475.
10. Sales, S.; Lourenço, H.M.; Bandarra, N.M.; Afonso, C.; Matos, J.; Botelho, M.J.; Pessoa, M.F.; Félix, P.M.; Veronez, A.; Cardoso, C. How Biological Activity in Sea Cucumbers Changes as a Function of Species and Tissue. *Foods* 2023, *13*, 35, doi:10.3390/foods13010035.
11. Feng, J.; Zhang, L.; Xia, X.; Hu, W.; Zhou, P. Effect of Geographic Variation on the Proteome of Sea Cucumber (Stichopus Japonicus). *Food Research International* 2020, *136*, 109498, doi:10.1016/j.foodres.2020.109498.
12. Nuringtyas, T.R.; Hidayati, L.; Rohmah, Z.; Paramita, D.K.; Suparmin, A.; Prinanda, H.H.; Febryzalita, Q.N.; Utami, S.L.; Zulfa, L.F.; Ardiansyah, B.K.; et al. Bioactive Peptides from Sea Cucumbers and Sea Urchins: Therapeutic Roles and Mechanistic Insights. *Trends in Sciences* 2025, *22*, 9513, doi:10.48048/tis.2025.9513.
13. Popov, A.; Kozlovskaya, E.; Rutckova, T.; Styshova, O.; Makhankov, V.; Vakhrushev, A.; Hushpulian, D.; Gazaryan, I.; Son, O.; Tekutyeva, L. Matrikines of Sea Cucumbers: Structure, Biological Activity and Mechanisms of Action. *Int J Mol Sci* 2024, *25*, 12068, doi:10.3390/ijms252212068.
14. Olivera-Castillo, L.; Grant, G.; Kantún-Moreno, N.; Barrera-Pérez, H.A.; Montero, J.; Olvera-Novoa, M.A.; Carrillo-Cocom, L.M.; Acevedo, J.J.; Puerto-Castillo, C.; May Solís, V.; et al. A Glycosaminoglycan-Rich Fraction from Sea Cucumber Isostichopus Badionotus Has Potent Anti-Inflammatory Properties In Vitro and In Vivo. *Nutrients* 2020, *12*, 1698, doi:10.3390/nu12061698.
15. Olivera-Castillo, L.; Grant, G.; Kantún-Moreno, N.; Acevedo-Fernández, J.J.; Puc-Sosa, M.; Montero, J.; Olvera-Novoa, M.A.; Negrete-León, E.; Santa-Olalla, J.; Ceballos-Zapata, J.; et al. Sea Cucumber (Isostichopus Badionotus) Body-Wall Preparations Exert Anti-Inflammatory Activity in Vivo. *PharmaNutrition* 2018, *6*, 74–80, doi:10.1016/j.phanu.2018.03.002.
16. Wiegand, C.; Dirksen, A.; Tittelbach, J. Treatment with a Red-laser-based Wound Therapy Device Exerts Positive Effects in Models of Delayed Keratinocyte and Fibroblast Wound Healing. *Photodermatol Photoimmunol Photomed* 2024, *40*, doi:10.1111/phpp.12926.
17. Kotian, S.R.; Bhat, K.M.R.; Padma, D.; Pai, K.S.R. Influence of Traditional Medicines on the Activity of Keratinocytes in Wound Healing: An *in-Vitro* Study. *Anat Cell Biol* 2019, *52*, 324, doi:10.5115/acb.19.009.
18. Sánchez-Solís, M.J.; Gullian-Klanian, M.; Toledo-López, V.; Lora-Vilchis, M.C.. Proximate composition and fatty acid profile of the sea cucumber isostichopus badionotus and holothuria floridana *Food Sci Technol Res* 2021, *27*, 319–327, doi:10.3136/fstr.27.319.
19. Acosta, E.J.; Rodríguez-Forero, A.; Werding, B.; Kunzmann, A. Ecological and Reproductive Characteristics of Holothuroids Isostichopus Badionotus and Isostichopus Sp. in Colombia. *PLoS One* 2021, *16*, e0247158, doi:10.1371/journal.pone.0247158.
20. Farooq, S.; Ahmad, M.I.; Zheng, S.; Ali, U.; Li, Y.; Shixiu, C.; Zhang, H. A Review on Marine Collagen: Sources, Extraction Methods, Colloids Properties, and Food Applications. *Collagen and Leather* 2024, *6*, 11, doi:10.1186/s42825-024-00152-y.
21. Karapanagiotidis, I.T.; Gkalogianni, E.Z.; Apostologamvrou, C.; Voulgaris, K.; Varkoulis, A.; Vafidis, D. Proximate Compositions and Fatty Acid Profiles of Raw and Processed Holothuria Polii and Holothuria Tubulosa from the Aegean Sea. *Sustainability* 2024, *16*, 6048, doi:10.3390/su16146048.

22. Talab et al., A.S. Proximate Composition and Quality Properties of Some Egyptian Sea Cucumber Species. *Egypt J Aquat Biol Fish* 2024, *28*, 379–396, doi:10.21608/EJABF.2024.338621.
23. Wen, Y.; Dong, X.; Zamora, L.N.; Jeffs, A.G.; Quek, S.Y. Physicochemical Properties, Functionalities, and Antioxidant Activity of Protein Extracts from New Zealand Wild Sea Cucumbers (Australostichopus Mollis). *Foods* 2024, *13*, 2735, doi:10.3390/foods13172735.
24. Muhsin, M.F.; Fujaya, Y.; Hidayani, A.A.; Fazhan, H.; Wan Mahari, W.A.; Lam, S.S.; Shu-Chien, A.C.; Wang, Y.; Afiqah-Aleng, N.; Rukminasari, N.; et al. Bridging the Gap between Sustainability and Profitability: Unveiling the Untapped Potential of Sea Cucumber Viscera. *PeerJ* 2023, *11*, e16252, doi:10.7717/peerj.16252.
25. Sugesti Yogi Pamungkas; Florensius Eko Dwi Haryono Bioprospecting of Sea Cucumber (Holothuria Sp.) as Industries and Functional Foods for Human Health. *International Journal of Science and Research Archive* 2023, *10*, 669–690, doi:10.30574/ijsra.2023.10.2.0994.
26. Purcell, S.W.; Lovatelli, A.; González-Wangüemert, M.; Solís-Marín, F.A.; Samyn, Y.; Conand, C. *Commercially Important Sea Cucumbers of the World*; No. 6, Rev. 1.; FAO: Rome, 2023; Vol. No. 6, Rev. 1; ISBN 978-92-5-137793-2.
27. Becerra, J.; Rodriguez, M.; Leal, D.; Noris-Suarez, K.; Gonzalez, G. Chitosan-Collagen-Hydroxyapatite Membranes for Tissue Engineering. *J Mater Sci Mater Med* 2022, *33*, 18, doi:10.1007/s10856-022-06643-w.
28. Teng, S.; Lee, E.; Wang, P.; Shin, D.; Kim, H. Three-layered Membranes of Collagen/Hydroxyapatite and Chitosan for Guided Bone Regeneration. *J Biomed Mater Res B Appl Biomater* 2008, *87B*, 132–138, doi:10.1002/jbm.b.31082.
29. Zheng, Z.; Sun, N.; Lu, Z.; Zheng, J.; Zhang, S.; Lin, S. The Potential Mechanisms of Skin Wound Healing Mediated by Tetrapeptides from Sea Cucumber. *Food Biosci* 2023, *53*, 102742, doi:10.1016/j.fbio.2023.102742.
30. Ibrahim, N. 'Izzah; Wong, S.K.; Mohamed, I.N.; Mohamed, N.; Chin, K.-Y.; Ima-Nirwana, S.; Shuid, A.N. Wound Healing Properties of Selected Natural Products. *Int J Environ Res Public Health* 2018, *15*, 2360, doi:10.3390/ijerph15112360.
31. Pérez-Vega, J.A.; Olivera-Castillo, L.; Gómez-Ruiz, J.Á.; Hernández-Ledesma, B. Release of Multifunctional Peptides by Gastrointestinal Digestion of Sea Cucumber (Isostichopus Badionotus). *J Funct Foods* 2013, *5*, 869–877, doi:10.1016/j.jff.2013.01.036.
32. Park, S.-Y.; Lim, H.K.; Lee, S.; Hwang, H.C.; Cho, S.K.; Cho, M. Pepsin-Solubilised Collagen (PSC) from Red Sea Cucumber (Stichopus Japonicus) Regulates Cell Cycle and the Fibronectin Synthesis in HaCaT Cell Migration. *Food Chem* 2012, *132*, 487–492, doi:10.1016/j.foodchem.2011.11.032.
33. Atanassova, M.R.; Mildenberger, J.; Hansen, M.D.; Tamm, T. Microstructure of Sea Cucumber Parastichopus Tremulus Peptide Hydrogels and Bioactivity in Caco-2 Cell Culture Model. *Gels* 2025, *11*, 280, doi:10.3390/gels11040280.
34. Man, J.; Abd El-Aty, A.M.; Wang, Z.; Tan, M. Recent Advances in Sea Cucumber Peptide: Production, Bioactive Properties, and Prospects. *Food Front* 2023, *4*, 131–163, doi:10.1002/fft2.196.
35. Senadheera, T.R.L.; Dave, D.; Shahidi, F. Antioxidant Potential and Physicochemical Properties of Protein Hydrolysates from Body Parts of North Atlantic Sea Cucumber (Cucumaria Frondosa). *Food Production, Processing and Nutrition* 2021, *3*, 3, doi:10.1186/s43014-020-00049-3.
36. Barzkar, N.; Attaran-Fariman, G.; Taheri, A.; Venmathi Maran, B.A. Extraction and Characterization of Collagen and Gelatin from Body Wall of Sea Cucumbers *Stichopus Horrens* and *Holothuria Arenicola*. *PeerJ* 2024, *12*, e18149, doi:10.7717/peerj.18149.
37. Nabilla, N.; Shofiyah, I.; Sugiharto; Alvitasari, D.; Sumarsih, S.; Khaleyla, F.; Wirawati, I.; Winarni, D. Organization, Density, and Content of Collagen in the Body Wall of Sea Cucumbers Acaudina Rosettis and Phyllophorus Sp. *Aquac Fish* 2024, doi:10.1016/j.aaf.2024.09.003.
38. Senadheera, T.R.L.; Dave, D.; Shahidi, F. Sea Cucumber Derived Type I Collagen: A Comprehensive Review. *Mar Drugs* 2020, *18*, 471, doi:10.3390/md18090471.
39. Liu, Y.; Zheng, Q.; Tan, M.; Chen, Z.; Zheng, H.; Gao, J.; Lin, H.; Zhu, G.; Cao, W. Characterization and Film-Forming Properties of Collagen from Three Species of Sea Cucumber from the South China Sea: Emphasizing the Effect of Transglutaminase. *Int J Biol Macromol* 2025, *294*, 139321, doi:10.1016/j.ijbiomac.2024.139321.

 doi:10.20944/preprints202509.1539.v1

40. Zhang, C.; Wang, W.; Li, H.; Che, H.; Xie, W.; Ju, W.; Qi, H.; Dong, X. Effect of Ca2+ on the Structure of Collagen Fibers in Sea Cucumber (Apostichopus Japonicus) under Low-Temperature Tenderization Condition. *Food Chem X* 2025, *27*, 102450, doi:10.1016/j.fochx.2025.102450.
41. Cruz-López, H.; Rodríguez-Morales, S.; Enríquez-Paredes, L.M.; Villarreal-Gómez, L.J.; True, C.; Olivera-Castillo, L.; Fernández-Velasco, D.A.; López, L.M. Swim Bladder of Farmed Totoaba Macdonaldi: A Source of Value-Added Collagen. *Mar Drugs* 2023, *21*, 173, doi:10.3390/md21030173.
42. Cruz-López, H.; Rodríguez-Morales, S.; Enríquez-Paredes, L.M.; Villarreal-Gómez, L.J.; Olivera-Castillo, L.; Cortes-Santiago, Y.; López, L.M. Comparison of Collagen Characteristic from the Skin and Swim Bladder of Gulf Corvina (Cynoscion Othonopterus). *Tissue Cell* 2021, *72*, 101593, doi:10.1016/j.tice.2021.101593.
43. Indriani, S.; Benjakul, S.; Quan, T.H.; Sitanggang, A.B.; Chaijan, M.; Kaewthong, P.; Petcharat, T.; Karnjanapratum, S. Effect of Different Ultrasound-Assisted Process Modes on Extraction Yield and Molecular Characteristics of Pepsin-Soluble Collagen from Asian Bullfrog Skin. *Food Bioproc Tech* 2023, *16*, 3019–3032, doi:10.1007/s11947-023-03118-w.
44. Li, P.-H.; Lu, W.-C.; Chan, Y.-J.; Ko, W.-C.; Jung, C.-C.; Le Huynh, D.T.; Ji, Y.-X. Extraction and Characterization of Collagen from Sea Cucumber (Holothuria Cinerascens) and Its Potential Application in Moisturizing Cosmetics. *Aquaculture* 2020, *515*, 734590, doi:10.1016/j.aquaculture.2019.734590.
45. Zhong, M.; Chen, T.; Hu, C.; Ren, C. Isolation and Characterization of Collagen from the Body Wall of Sea Cucumber *Stichopus Monotuberculatus*. *J Food Sci* 2015, *80*, doi:10.1111/1750-3841.12826.
46. Liu, Z.; Oliveira, A.C.M.; Su, Y.-C. Purification and Characterization of Pepsin-Solubilized Collagen from Skin and Connective Tissue of Giant Red Sea Cucumber (Parastichopus Californicus). *J Agric Food Chem* 2010, *58*, 1270–1274, doi:10.1021/jf9032415.
47. Zhu, L.; Wang, W.; Meng, Y.; Tian, Q.; Hao, L.; Hou, H. Thermal Stability of Sea Cucumber Collagen and Effects of Gallic Acid Crosslinking. *Int J Food Sci Technol* 2023, *58*, 2280–2288, doi:10.1111/ijfs.16347.
48. Lu, Z.; Sun, N.; Dong, L.; Gao, Y.; Lin, S. Production of Bioactive Peptides from Sea Cucumber and Its Potential Health Benefits: A Comprehensive Review. *J Agric Food Chem* 2022, *70*, 7607–7625, doi:10.1021/acs.jafc.2c02696.
49. Yang, F.; Bai, X.; Dai, X.; Li, Y. The Biological Processes During Wound Healing. *Regenerative Med* 2021, *16*, 373–390, doi:10.2217/rme-2020-0066.
50. Martinotti, S.; Ranzato, E. Scratch Wound Healing Assay. In *Methods Mol Biol*; 2019; Vol. 2109, pp. 225–229, doi:10.1007/7651_2019_259
51. Aw, Y.B.; Chen, S.; Yeo, A.; Dangerfield, J.A.; Mok, P. Development and Functional Testing of a Novel in Vitro Delayed Scratch Closure Assay. *Histochem Cell Biol* 2024, *162*, 245–255, doi:10.1007/s00418-024-02292-y.
52. Wiegand, C.; Hipler, U.-C.; Elsner, P.; Tittelbach, J. Keratinocyte and Fibroblast Wound Healing In Vitro Is Repressed by Non-Optimal Conditions but the Reparative Potential Can Be Improved by Water-Filtered Infrared A. *Biomedicines* 2021, *9*, 1802, doi:10.3390/biomedicines9121802.
53. Farhangniya, M.; Samadikuchaksaraei, A. A Review of Genes Involved in Wound Healing. *Med J Islam Repub Iran* 2023, doi:10.47176/mjiri.37.140.
54. Morgner, B.; Husmark, J.; Arvidsson, A.; Wiegand, C. Effect of a DACC-Coated Dressing on Keratinocytes and Fibroblasts in Wound Healing Using an in Vitro Scratch Model. *J Mater Sci Mater Med* 2022, *33*, 22, doi:10.1007/s10856-022-06648-5.
55. Ågren, M.S.; Litman, T.; Eriksen, J.O.; Schjerling, P.; Bzorek, M.; Gjerdrum, L.M.R. Gene Expression Linked to Reepithelialization of Human Skin Wounds. *Int J Mol Sci* 2022, *23*, 15746, doi:10.3390/ijms232415746.
56. Costantini, E.; Aielli, L.; Serra, F.; De Dominicis, L.; Falasca, K.; Di Giovanni, P.; Reale, M. Evaluation of Cell Migration and Cytokines Expression Changes under the Radiofrequency Electromagnetic Field on Wound Healing In Vitro Model. *Int J Mol Sci* 2022, *23*, 2205, doi:10.3390/ijms23042205.
57. Marinelli, L.; Cacciatore, I.; Costantini, E.; Dimmito, M.P.; Serra, F.; Di Stefano, A.; Reale, M. Wound-Healing Promotion and Anti-Inflammatory Properties of Carvacrol Prodrugs/Hyaluronic Acid Formulations. *Pharmaceutics* 2022, *14*, 1468, doi:10.3390/pharmaceutics14071468.

 doi:10.20944/preprints202509.1539.v1

58. Kawano, Y.; Patrulea, V.; Sublet, E.; Borchard, G.; Iyoda, T.; Kageyama, R.; Morita, A.; Seino, S.; Yoshida, H.; Jordan, O.; et al. Wound Healing Promotion by Hyaluronic Acid: Effect of Molecular Weight on Gene Expression and In Vivo Wound Closure. *Pharmaceuticals* 2021, *14*, 301, doi:10.3390/ph14040301.
59. Yuksel, S.N.; Dikmen, M.; Canturk, Z. Evaluation of Real Time Cell Proliferation, Anti-Inflammatory and Wound Healing Potential of Helenalin on HaCaT Keratinocytes Treated with Lipopolysaccharide Stimulated Monocytes. *Indian J Pharm Sci* 2021, doi:10.36468/pharmaceutical-sciences.767.
60. Shamilov, R.; Ackley, T.W.; Aneskievich, B.J. Enhanced Wound Healing- and Inflammasome-Associated Gene Expression in TNFAIP3-Interacting Protein 1- (TNIP1-) Deficient HaCaT Keratinocytes Parallels Reduced Reepithelialization. *Mediators Inflamm* 2020, *2020*, 1–14, doi:10.1155/2020/5919150.
61. Patruno, A.; Ferrone, A.; Costantini, E.; Franceschelli, S.; Pesce, M.; Speranza, L.; Amerio, P.; D'Angelo, C.; Felaco, M.; Grilli, A.; et al. Extremely Low-frequency Electromagnetic Fields Accelerates Wound Healing Modulating <scp>MMP</Scp> -9 and Inflammatory Cytokines. *Cell Prolif* 2018, *51*, doi:10.1111/cpr.12432.
62. Peplow, P. V.; Chatterjee, M.P. A Review of the Influence of Growth Factors and Cytokines in In Vitro Human Keratinocyte Migration. *Cytokine* 2013, *62*, 1–21, doi:10.1016/j.cyto.2013.02.015.
63. Koivisto, L.; Jiang, G.; Häkkinen, L.; Chan, B.; Larjava, H. HaCaT Keratinocyte Migration Is Dependent on Epidermal Growth Factor Receptor Signaling and Glycogen Synthase Kinase-3α. *Exp Cell Res* 2006, *312*, 2791–2805, doi:10.1016/j.yexcr.2006.05.009.
64. Geahchan, S.; Baharlouei, P.; Rahman, A. Marine Collagen: A Promising Biomaterial for Wound Healing, Skin Anti-Aging, and Bone Regeneration. *Mar Drugs* 2022, *20*, 61, doi:10.3390/md20010061.
65. Comino-Sanz, I.M.; López-Franco, M.D.; Castro, B.; Pancorbo-Hidalgo, P.L. The Role of Antioxidants on Wound Healing: A Review of the Current Evidence. *J Clin Med* 2021, *10*, 3558, doi:10.3390/jcm10163558.
66. Lu, W.; Shi, Y.; Wang, R.; Su, D.; Tang, M.; Liu, Y.; Li, Z. Antioxidant Activity and Healthy Benefits of Natural Pigments in Fruits: A Review. *Int J Mol Sci* 2021, *22*, 4945, doi:10.3390/ijms22094945.
67. Yang, C.S.; Ho, C.-T.; Zhang, J.; Wan, X.; Zhang, K.; Lim, J. Antioxidants: Differing Meanings in Food Science and Health Science. *J Agric Food Chem* 2018, *66*, 3063–3068, doi:10.1021/acs.jafc.7b05830.
68. Mfotie Njoya, E. Medicinal Plants, Antioxidant Potential, and Cancer. In *Cancer*; Preedy, V.R., Patel, V.B., Eds.; Elsevier, 2021; pp. 349–357.
69. Sakurai, S.; Kawakami, Y.; Kuroki, M.; Gotoh, H. Structure–Antioxidant Activity (Oxygen Radical Absorbance Capacity) Relationships of Phenolic Compounds. *Struct Chem* 2022, *33*, 1055–1062, doi:10.1007/s11224-022-01920-4.
70. Mathew-Steiner, S.S.; Roy, S.; Sen, C.K. Collagen in Wound Healing. *Bioengineering* 2021, *8*, 63, doi:10.3390/bioengineering8050063.
71. Rowley, A.T.; Meli, V.S.; Wu-Woods, N.J.; Chen, E.Y.; Liu, W.F.; Wang, S.-W. Effects of Surface-Bound Collagen-Mimetic Peptides on Macrophage Uptake and Immunomodulation. *Front Bioeng Biotechnol* 2020, *8*, doi:10.3389/fbioe.2020.00747.
72. Szarka, E.; Neer, Z.; Balogh, P.; Ádori, M.; Angyal, A.; Prechl, J.; Kiss, A.; Kövesdi, D.; Sármay, G. Exacerbation of Collagen Induced Arthritis by FcΓ Receptor Targeted Collagen Peptide Due to Enhanced Inflammatory Chemokine and Cytokine Production. *Biologics* 2012, *6*, 101–115, doi:10.2147/BTT.S29749.
73. Pilus, N.S.M.; Muhamad, A.; Shahidan, M.A.; Yusof, N.Y.M. Potential of Epidermal Growth Factor-like Peptide from the Sea Cucumber Stichopus Horrens to Increase the Growth of Human Cells: In Silico Molecular Docking Approach. *Mar Drugs* 2022, *20*, 596, doi:10.3390/md20100596.
74. Sun, J.-H.; Song, S.; Yang, J.-F. Oral Administration of Sea Cucumber (*Stichopus Japonicus*) Protein Exerts Wound Healing Effects *via* the PI3K/AKT/MTOR Signaling Pathway. *Food Funct* 2022, *13*, 9796–9809, doi:10.1039/D2FO01372J.
75. Laemmli, U.K. Cleavage of Structural Proteins during the Assembly of the Head of Bacteriophage T4. *Nature* 1970, *227*, 680–685, doi:10.1038/227680a0.
76. Hagiwara, M. Sodium Dodecyl Sulfate-Polyacrylamide Gel Electrophoresis and Western Blotting Analyses via Colored Stacking Gels. *Anal Biochem* 2022, *652*, 114751, doi:10.1016/j.ab.2022.114751.

77. Chotphruethipong, L.; Binlateh, T.; Hutamekalin, P.; Aluko, R.E.; Tepaamorndech, S.; Zhang, B.; Benjakul, S. Impact of Hydrolyzed Collagen from Defatted Sea Bass Skin on Proliferation and Differentiation of Preosteoblast MC3T3-E1 Cells. *Foods* 2021, *10*, 1476, doi:10.3390/foods10071476.
78. Vieira, R.P.; Mourão, P.A. Occurrence of a Unique Fucose-Branched Chondroitin Sulfate in the Body Wall of a Sea Cucumber. *Journal of Biological Chemistry* 1988, *263*, 18176–18183, doi:10.1016/S0021-9258(19)81341-8.
79. Nielsen, P.M.; Petersen, D.; Dambmann, C. Improved Method for Determining Food Protein Degree of Hydrolysis. *J Food Sci* 2001, *66*, 642–646, doi:10.1111/j.1365-2621.2001.tb04614.x.
80. Spellman, D.; McEvoy, E.; O'Cuinn, G.; FitzGerald, R.J. Proteinase and Exopeptidase Hydrolysis of Whey Protein: Comparison of the TNBS, OPA and PH Stat Methods for Quantification of Degree of Hydrolysis. *Int Dairy J* 2003, *13*, 447–453, doi:10.1016/S0958-6946(03)00053-0.
81. Hernández-Ledesma, B.; Miralles, B.; Amigo, L.; Ramos, M.; Recio, I. Identification of Antioxidant and ACE-inhibitory Peptides in Fermented Milk. *J Sci Food Agric* 2005, *85*, 1041–1048, doi:10.1002/jsfa.2063.
82. Garrett, A.R.; Weagel, E.G.; Martinez, A.D.; Heaton, M.; Robison, R.A.; O'Neill, K.L. A Novel Method for Predicting Antioxidant Activity Based on Amino Acid Structure. *Food Chem* 2014, *158*, 490–496, doi:10.1016/j.foodchem.2014.02.102.
83. Mani, S.; Swargiary, G. In Vitro Cytotoxicity Analysis: MTT/XTT, Trypan Blue Exclusion. In; 2023; pp. 267–284.
84. Nagy, G.; Kiraly, G.; Banfalvi, G. Optimization of Cell Cycle Measurement by Time-Lapse Microscopy. In *Methods in Cell Biology*; P. Michael Conn, Ed.; Academic Press, 2012; Vol. 112, pp. 143–161.
85. Wallace, S.E.; Wilcox, W.R. *Camurati-Engelmann Disease*; Adam MP, Feldman J, Mirzaa GM, Pagon RA, Wallace SE, Amemiya A, Eds.; GeneReviews® [Internet]: Seattle (WA): , 2023;
86. Rebrikov, D. V.; Trofimov, D.Yu. Real-Time PCR: A Review of Approaches to Data Analysis. *Appl Biochem Microbiol* 2006, *42*, 455–463, doi:10.1134/S0003683806050024.
87. Livak, K.J.; Schmittgen, T.D. Analysis of Relative Gene Expression Data Using Real-Time Quantitative PCR and the 2−ΔΔCT Method. *Methods* 2001, *25*, 402–408, doi:10.1006/meth.2001.1262.
88. Pfaffl, M.W. A New Mathematical Model for Relative Quantification in Real-Time RT-PCR. *Nucleic Acids Res* 2001, *29*, 45e–445, doi:10.1093/nar/29.9.e45.
89. Artika, I.M.; Dewi, Y.P.; Nainggolan, I.M.; Siregar, J.E.; Antonjaya, U. Real-Time Polymerase Chain Reaction: Current Techniques, Applications, and Role in COVID-19 Diagnosis. *Genes (Basel)* 2022, *13*, 2387, doi:10.3390/genes13122387.